ASD-TDR-62-69

RESEARCH ON SOLAR-ENERGY CONVERSION EMPLOYING CADMIUM SULFIDE

TECHNICAL DOCUMENTARY REPORT NO. ASD-TDR-62-69

June 1962

Flight Accessories Laboratory
Aeronautical Systems Division
Air Force Systems Command
Wright-Patterson Air Force Base, Ohio

Project No. 3145, Task No. 314508

(Prepared under Contract No. AF 33(616)-7528
by Solid State Research & Electronics Division,
The Harshaw Chemical Company, Cleveland, Ohio
Authors: Fred A. Shirland, G. A. Wolff and John D. Nixon)

Aeronautical Systems Division, Dir/Aeromechanics, Flight Accessories Lab, Wright-Patterson AFB, Ohio. Rpt Nr ASD-TDR-62-69. RESEARCH ON SOLAR-ENERGY CONVERSION EMPLOYING CADMIUM SULFIDE. Summary report, June 62, 73p. incl illus., tables, 25 refs.

Unclassified Report

Application of CdS to photovoltaic conversion has been continued with primary emphasis on cells fabricated from vacuum evaporated CdS films. Back wall CdS film cells on conducting glass substrates have given efficiencies up to 5% on small areas. Front wall CdS film cells on molybdenum foil substrates have given efficiencies up to 2.5% on small areas and up to 1.0% on larger areas of 9 in^2. Thin lightweight arrays have been constructed from the latter cells having power to

(over)

weight ratios up to 10 watts per pound. Improvements promising increases up to 30 to 40 watts per pound are discussed. Arrays of CdS film cells of 1 square foot area have been constructed. Fundamental investigations were initiated on the growth, annealing, etching, and orientation of CdS single crystals and films. The results were correlated with the type of crystal imperfection and its probable influences on electrical properties. The photovoltaic barrier was studied experimentally to identify the essential constituents and to improve the expected efficiency of energy conversion. Theoretical models were postulated for the mechanisms occurring in the CdS photovoltaic cell.

1. Solar cells
2. Photovoltaic materials
3. Solar energy conversion
4. Semiconductors

I. AFSC Project 3145, Task 314508
II. Contract AF33(616)-7528
III. Harshaw Chem. Co., 2240 Prospect Ave., Cleveland 15, Ohio
IV. F.A. Shirland, G.A. Wolff and J.D. Nixon
V. Aval fr OTS
VI. In ASTIA collection

Aeronautical Systems Division, Dir/Aeromechanics, Flight Accessories Lab, Wright-Patterson AFB, Ohio. Rpt Nr ASD-TDR-62-69. RESEARCH ON SOLAR-ENERGY CONVERSION EMPLOYING CADMIUM SULFIDE. Summary report, June 62, 73p. incl illus., tables, 25 refs.

Unclassified Report

Application of CdS to photovoltaic conversion has been continued with primary emphasis on cells fabricated from vacuum evaporated CdS films. Back wall CdS film cells on conducting glass substrates have given efficiencies up to 5% on small areas. Front wall CdS film cells on molybdenum foil substrates have given efficiencies up to 2.5% on small areas and up to 1.0% on larger areas of 9 in^2. Thin lightweight arrays have been constructed from the latter cells having power to

(over)

weight ratios up to 10 watts per pound. Improvements promising increases up to 30 to 40 watts per pound are discussed. Arrays of CdS film cells of 1 square foot area have been constructed. Fundamental investigations were initiated on the growth, annealing, etching, and orientation of CdS single crystals and films. The results were correlated with the type of crystal imperfection and its probable influences on electrical properties. The photovoltaic barrier was studied experimentally to identify the essential constituents and to improve the expected efficiency of energy conversion. Theoretical models were postulated for the mechanisms occurring in the CdS photovoltaic cell.

1. Solar cells
2. Photovoltaic materials
3. Solar energy conversion
4. Semiconductors

I. AFSC Project 3145, Task 314508
II. Contract AF33(616)-7528
III. Harshaw Chem. Co., 2240 Prospect Ave., Cleveland 15, Ohio
IV. F.A. Shirland, G.A. Wolff and J.D. Nixon
V. Aval fr OTS
VI. In ASTIA collection

Aeronautical Systems Division, Dir/Aeromechanics, Flight Accessories Lab, Wright-Patterson AFB, Ohio. Rpt Nr ASD-TDR-62-69. RESEARCH ON SOLAR-ENERGY CONVERSION EMPLOYING CADMIUM SULFIDE. Summary report, June 62, 73p. incl illus., tables, 25 refs.

Unclassified Report

Application of CdS to photovoltaic conversion has been continued with primary emphasis on cells fabricated from vacuum evaporated CdS films. Back wall CdS film cells on conducting glass substrates have given efficiencies up to 5% on small areas. Front wall CdS film cells on molybdenum foil substrates have given efficiencies up to 2.5% on small areas and up to 1.0% on larger areas of 9 in^2. Thin lightweight arrays have been constructed from the latter cells having power to

(over)

weight ratios up to 10 watts per pound. Improvements promising increases up to 30 to 40 watts per pound are discussed. Arrays of CdS film cells of 1 square foot area have been constructed. Fundamental investigations were initiated on the growth, annealing, etching, and orientation of CdS single crystals and films. The results were correlated with the type of crystal imperfection and its probable influences on electrical properties. The photovoltaic barrier was studied experimentally to identify the essential constituents and to improve the expected efficiency of energy conversion. Theoretical models were postulated for the mechanisms occurring in the CdS photovoltaic cell.

1. Solar cells
2. Photovoltaic materials
3. Solar energy conversion
4. Semiconductors

I. AFSC Project 3145, Task 314508
II. Contract AF33(616)-7528
III. Harshaw Chem. Co., 2240 Prospect Ave., Cleveland 15, Ohio
IV. F.A. Shirland, G.A. Wolff and J.D. Nixon
V. Aval fr OTS
VI. In ASTIA collection

Aeronautical Systems Division, Dir/Aeromechanics, Flight Accessories Lab, Wright-Patterson AFB, Ohio. Rpt Nr ASD-TDR-62-69. RESEARCH ON SOLAR-ENERGY CONVERSION EMPLOYING CADMIUM SULFIDE. Summary report, June 62, 73p. incl illus., tables, 25 refs.

Unclassified Report

Application of CdS to photovoltaic conversion has been continued with primary emphasis on cells fabricated from vacuum evaporated CdS films. Back wall CdS film cells on conducting glass substrates have given efficiencies up to 5% on small areas. Front wall CdS film cells on molybdenum foil substrates have given efficiencies up to 2.5% on small areas and up to 1.0% on larger areas of 9 in^2. Thin lightweight arrays have been constructed from the latter cells having power to

(over)

weight ratios up to 10 watts per pound. Improvements promising increases up to 30 to 40 watts per pound are discussed. Arrays of CdS film cells of 1 square foot area have been constructed. Fundamental investigations were initiated on the growth, annealing, etching, and orientation of CdS single crystals and films. The results were correlated with the type of crystal imperfection and its probable influences on electrical properties. The photovoltaic barrier was studied experimentally to identify the essential constituents and to improve the expected efficiency of energy conversion. Theoretical models were postulated for the mechanisms occurring in the CdS photovoltaic cell.

1. Solar cells
2. Photovoltaic materials
3. Solar energy conversion
4. Semiconductors

I. AFSC Project 3145, Task 314508
II. Contract AF33(616)-7528
III. Harshaw Chem. Co., 2240 Prospect Ave., Cleveland 15, Ohio
IV. F.A. Shirland, G.A. Wolff and J.D. Nixon
V. Aval fr OTS
VI. In ASTIA collection

[illegible] WPAFB Ltr. 1960-37236

FOREWORD

ASD-TDR-62-69

This report was prepared by The Harshaw Chemical Company, Solid State Research Laboratories, as a summary report covering the research and development on Contract AF33(616)-7528, Project No. 1(3-3145), Task No. 314508. The project was funded by the Flight Accessories Lab of ASD, initiated by the Aeronautical Research Laboratory. Mr. Donald C. Reynolds acted as Contract Monitor with Mr. Joseph Wise representing ASD.

This contract is concerned with the work from July 1960 through December 1961. The following technical personnel have contributed to the project during the period of Contract AF33(616)-7528: F. A. Shirland, G. A. Wolff, J. D. Nixon, J. D. Broder, G. H. Dierssen, J. Frawley, O. G. Fritz, T. A. Griffin, E. R. Hill, J. Harpster, N. E. Heyerdahl, J. R. Hietanen, F. N. Lancia, A. E. Middleton, and H. E. Nastelin. Project direction has been provided by F. A. Shirland. During the last half of the project, the basic supporting research has been separated from the development aspects and has been coordinated by G. A. Wolff.

Acknowledgment is made to Dr. A. E. Middleton who has provided overall direction of the work of this and related projects as Director and Manager of the Solid State Research Laboratories of The Harshaw Chemical Company, and to Dr. Richard W. Hoffman of The Case Institute of Technology, who was consulted on problems concerning the vacuum evaporation of CdS films.

ABSTRACT

Application of semi-conductive CdS to photovoltaic energy conversion has been continued with primary emphasis on cells fabricated from vacuum evaporated CdS films. Back wall CdS film cells on conducting glass substrates have given conversion efficiencies up to 5% on small areas. Front wall CdS film cells on molybdenum foil substrates have given conversion efficiencies up to 2.5% on small areas and up to 1.0% on larger areas of 9 in^2. Thin light weight arrays have been constructed from these latter cells giving power to weight ratios up to 10 watts per pound. Possible improvements promising increases of the ratio up to 30 to 40 watts per pound are discussed. Arrays of CdS film cells of 1 square foot area have been constructed.

Fundamental investigations were initiated on the growth, annealing, etching and orientation of CdS single crystals and films. The results were correlated with the type of crystal imperfection and its probable influences on electrical properties. The photovoltaic barrier was studied experimentally to identify the essential constituents and to improve the expected efficiency of energy conversion. Theoretical models were postulated for the mechanisms occurring in the CdS photovoltaic cell. The predicted behavior was compared with actual operation.

TABLE OF CONTENTS

Page

PART I - DEVELOPMENT

INTRODUCTION 1

RAW MATERIALS 1
- G. E. Luminescent Grade CdS 1
- Other Materials 1
- Purity Considerations 3

CRYSTAL GROWTH 7
- Equipment 7
- Growth Runs 7
- Vacuum Growth 9
- H_2S Atmosphere Growth 10
- Homogeneity 11

FILM CELLS 12
- General 12
- Backwall Cell 15
  - Process 15
  - Performance 16
- Lightweight Cell 18
- Front Wall Cell 21
  - Front vs Back Wall Operation 21
  - Process 23
  - Performance 23
  - Cell Size 26
  - Surface Preparation 27
  - Multiple Evaporation 27

ARRAYS 28
- Design and Equipment 28
- Materials 30
- Results 31

TEST DATA 34
- Temperature 34
- Stability 34

PART II - BASIC SUPPORTING RESEARCH

OBJECTIVES 40

SINGLE CRYSTAL AND FILM STUDIES 40
- Single Crystal Growth and Annealing 40
- Etching and Orientation Studies on Single Crystals 41
- Grain Growth of CdS Films 45
- Dislocation Studies and Etching Behavior 45

Table of Contents (Continued)

Page

EXPERIMENTAL WORK ON THE PHOTOVOLTAIC BARRIER 52
- Analysis for Copper at Various Stages of Cell Formation . . . 52
- Deposition of Copper by Various Methods 55
- Other Investigations on the Nature of the Barrier 56
  - Statement of the Problem 56
  - Supporting Experimental Data 57
- Summary of Surface Reactions 60

THEORETICAL STUDY OF THE PHOTOVOLTAIC CELL 60
- Theory of the Surface Barrier Photovoltaic Effect 60
- A Hypothesis on Injecting Contacts 65
- Applications to the CdS Photovoltaic Cell 67
- The Barrier Capacity 69
- Summary of Cell Operation 69

PART III - RECOMMENDATIONS 70

REFERENCE LIST 72

LIST OF FIGURES

Figure Title Page

1 Vapor Phase Growth Facilities for CdS 8

2 Enlarged View of Backwall CdS Film Cell Showing Construction 17

3 Backwall vs Frontwall Spectral Response 22

4 Effect of CdS Film Thickness on Light and Dark I-V Characteristic Curves 25

5 Layout of Array in Laminating Die Prior to Lamination 29

6 1 Square Foot CdS Film Cell Array and Several 6" x 6" Arrays, 3" x 3" Arrays and 1 - 1" x 3" Array 33

7 I-V Characteristic Curve - Evaporated CdS Film Cell on Glass 35

8 Open Circuit Voltage vs Temperature - CdS Evaporated Film Cell on Glass Substrate 36

9 Short Circuit Current vs Temperature - CdS Evaporated Film Cell on Glass Substrate 37

10 Output Power and Voc^{x} Isc vs Temperature - Evaporated Film Cell on Glass 38

11 Stereographic Projection of the Most Slowly Attacked Planes in Wurtzite Structure Materials 43

12 Light and Dark I-V Characteristic Curves for CdS Cells with Barriers on (0001) and (000$\bar{1}$) Surfaces. 44

13 Etched CdS Crystal Showing Dislocations 47

14 Etched CdS Crystal Showing Dendritic Structure 47

15 60° Dislocations, α and β Types, in CdS. 49

16 "Neutral" Dislocations in CdS 49

17 Solution Form Photomicrograph of CdS 50

18 Schematic Drawing of Rounded Solution Form and Corresponding Polyhedral Etch Pit Form in CdS 51

List of Illustrations (Cont'd)

Figure	Title	Page
19	Stereographic Projections Representing Both Rounded and Polyhedral Etch Pit Forms in CdS	51
20	Stereographic Projection and Clinographic Projection of Crystal Forms of Wurtzite Structure for the Various Ratios of Anionic to Cationic Contribution to the Surface (or Interface) Free Energy	53
21	Energy Level Diagram-Surface Barrier Photovoltaic Cell	62

LIST OF TABLES

Table	Title	Page
I	Emission Spectrographic Analyses of CdS Raw Materials	2
II	Neutron Activation Analyses of CdS Samples	4
III	Mass Spectrographic Analyses of CdS Samples	5
IV	Electrical Measurements on Consecutive Slices of .003% $InCl_3$ - Doped CdS	13
V	Electrical Measurements on Consecutive Slices of Undoped CdS	14
VI	Preliminary Evaluation of Various Possible Light Weight Substrates for Evaporated CdS Films	19
VII	The Analysis of the CdS and Plating Solution, Following Plating from a Cu Bath and Heating	54

INTRODUCTION

ASD-TDR-62-69

The following report summarizes the applied Research and Development work sponsored by the Air Force Systems Command and the Flight Accessories Laboratory of the United States Air Force at The Harshaw Chemical Company on semi-conductive CdS for photovoltaic energy conversion with single crystal and polycrystalline films for the period from July 1960 through December 1961.

Previous reports, WADC Technical Report No. 57-770, December 1957 and ARL Technical Report 60-293, August 1960, summarized the work prior to this time. Quarterly Progress Reports submitted to the Contract Monitor have covered the research and development findings in greater detail than is possible in a summary report.

This report is an interim summary report. Plans are being made for continuation of the work of materials research and device development.

PART I DEVELOPMENT

RAW MATERIALS

G. E. Luminescent Grade CdS

General Electric Company's luminescent grade CdS powder has been used as the raw material for most of the work of the past 18 months on the subject contract. Two new lots of this material have been procured during this period, but most of the work has been done with one lot, No. 69. The spectrographic analyses for these lots are given in Table I. The analyzed impurity content is comparable to that obtained on previous lots of General Electric material.(1)

Not shown in the analyses of Table I were appreciable amounts of certain alkali metal and alkaline earth impurities including sodium, lithium, and calcium, which were first detected from mass spectrographic analyses and subsequently verified by extending the emission spectrographic analysis spectrum from the UV to the visible region. These alkali metals have now also been found in the previous lots when analyzed by the revised technique.

Other Materials

Several other sources of CdS powder have been procured and evaluated during this period including Sylvania's luminescent grade CdS. Eagle-Picher Company's ultra pure CdS, and a luminescent grade material from E. Merck Company.

Manuscript released by the authors December 1961 for publication as an ASD Technical Documentary Report.

TABLE I

EMISSION SPECTROGRAPHIC ANALYSES OF CdS RAW MATERIALS

Source	Lot	Al	Cu	In	Fe	Pb	Mg	Mn	Ni	Ag	Zn	Mo
G. E.	69	VFT	VFT	-	FT/VFT	-	VFT	-	-	-	T-	VFT
	104	VFT+	VFT /VFT+	-	VFT+/FT	-	FT-	VFT	-	-	T+/W	-
Sylvania	C-676	VFT	VFT	-	VFT	-	FT	-	-	VFT	W-	-
	C-708	VFT	VFT-	-	VFT-	-	VFT+	-	-	FT-	W-	-
	C-716	VFT-	-	-	VFT-	-	VFT	-	-	VFT-	W+	-
E. Merck	P-4781	VFT	VFT	-	VFT	T-	VFT-	-	-	-	-	-

Key:
W = Weak - Approx. .01 to .1%
T = Trace - Approx. .001 to .01%
FT = Faint Trace
VFT = Very Faint Trace
\- = Not Detected

The spectrographic analyses of these materials also are given in Table I. It is difficult to be certain that these very slight indications from spectrographic analyses represent really significant differences of impurities. The emission spectrographic analysis test is operating at the limit of its capabilities for the barely detectable amounts of these impurities. All of the CdS lots listed in Table I are essentially comparable as far as indicated purity is concerned. In general, we have been unable to correlate the indicated variations in level of these barely detectable impurities with any physical, optical or electrical properties of the CdS crystals or cells made from these materials.

Purity Considerations

The reason that it has not been possible to observe a correlative relationship between the spectrographically indicated trace impurities in various CdS materials and crystal or cell properties may well be because such affects are masked by other impurities or imperfections present in larger amounts. Emission spectrographic analysis is a well established and useful technique for studies of certain impurities in various materials. However, it has limitations in that it is insensitive for some impurities that can be electrically important in semiconductors. Also it is not sensitive enough for some other impurities that can be detected by this method.

It is necessary therefore to supplement the obtainable data from the emission spectrograph by information from other methods of analysis. Some work has been carried out along these lines during this contract. Samples of CdS have been submitted for neutron activation analysis and also for mass spectrographic analysis. These other methods have shed considerable light upon the accuracy of the emission spectrograph and on the presence of other impurities that the emission spectrograph missed entirely.

Nearly all of the emission spectrographic analyses of CdS powder and CdS crystals from all sources available to The Harshaw Chemical Company have shown at least a VFT or VFT- of copper, aluminum, iron and magnesium. Occasionally silver and lead have also been detected. However, of a total of nine CdS samples, (four from Harshaw and five from the Eagle-Picher Company) that were submitted to Oakridge National Laboratory for neutron activation analyses not a single sample showed as much as 0.02 ppm of copper nor as much as 0.2 ppm of silver. These samples included both Eagle-Picher synthesized CdS raw material and General Electric Company's luminescent grade CdS raw material. These data are presented in Table II.

Also, of two Harshaw and two Eagle-Picher samples of CdS submitted to the Bell & Howell Research Center for mass spectrographic analysis, one sample of Eagle-Picher material showed 1 ppm of copper while the other three showed none, and none of the four showed any silver present. One of the Eagle-Picher samples showed 10 ppm of aluminum but the other three showed no aluminum. These data are presented in Table III. It does appear that the indications of copper, aluminum and possibly silver that are normally found in the CdS as very faint traces by emission spectrographic analysis are probably spurious, and that these

TABLE II

NEUTRON ACTIVATION ANALYSES OF CdS SAMPLES

Element Concentration - ppm by weight

Sample	Doping	Cu	Si	Ag	In***	Cl
A - CdS Raw Material	None	$<0.02^{*}$	$<10.^{**}$	$<0.2^{**}$	2,3	$<0.08^{*}$
B - CdS Crystal, G.E. Mat'l	.02% In_2S_3	$<0.02^{*}$	$<10.^{*}$	$<0.2^{**}$	0.04,0.03	$<0.08^{*}$
C - CdS Crystal, G.E. Mat'l	.003 $InCl_3$	$<0.02^{*}$	$<10.^{*}$	$<0.2^{**}$	2,3	$<0.08^{*}$
D - CdS Crystal, G.E. Mat'l	.003 $InCl_3$	$<0.02^{*}$	$<10.^{*}$	$<0.2^{**}$	31,40	$<0.08^{*}$
M 5903-BO		$<0.02^{*}$	-	$<0.2^{**}$	5.0,5.5	$<0.01^{*}$
-BQ		$<0.02^{*}$	-	$<0.2^{**}$	16.3,16.	$\leq 0.01^{*}$
-BN		$<0.02^{*}$	-	$<0.2^{**}$	7.7,7.5	$\leq 0.01^{*}$
-BP		$<0.02^{*}$	-	$<0.2^{**}$	1.7,1.8	$\leq 0.01^{*}$
-AE		$<0.02^{*}$	-	$<0.2^{**}$	2.3,2.0	$\leq 0.006^{*}$

NOTES:

Analyses by Oak Ridge National Laboratory - G. W. Leddicotte

Samples A,B,C, & D submitted by Harshaw - sample identities evidently were mixed as indicated by indium analyses.

Last 5 samples submitted by Eagle-Picher Co. - identity of material and doping not known at Harshaw, all were probably deliberately indium doped.

* Radioactivity detected - amount less than (indicated) measurement limit.

** Radioactivity not detected - limit of measurement indicated.

*** Two determinations made on each sample.

TABLE III

MASS SPECTROGRAPHIC ANALYSES OF CdS SAMPLES - ppm-atomic

Sample	Doping	Li	C	N	F	Na	Mg	Al	Si	Cl	K	Ca	Cu	In	Ru
Commercial E-P CdS		100	3	<3		3% *	10	10	100	1	10	10	1	5	10
E-P CdS Single Crystal M-6105-CZ			100	<10		300			<3		5	5			
Harshaw CdS Crystal 16-28P	None	300	10	<3		300			<10		30	2			
Harshaw CdS Crystal 16-18P	.003% $InCl_3$	5	15	<5	<.5	15			<15	1	.5	<.5		5	

NOTES: Semi-quantitative analyses made by Bell & Howell Research Center - R. K. W'llardson

Analyses made by visual comparison of line densities believed accurate only to a factor of 3. The doping of the Eagle-Picher samples, and the type of starting raw material is not known at this laboratory.

Blanks are assumed to indicate that the element was looked for but not detected, while those showing less than some amount are assumed to have been detected but below the (stated) measurement limit. Other elements presumably looked for but not detected in the above 4 samples are P, Ni, As, Se, Mo and Ag.

* As reported by analyst. Unbelievably high value probably represents extraneous contamination of sample - corroboration by re-sampling not attempted.

impurities are usually below the limit of detection by this method.

The mass spectrograph indicated the presence of some impurities that were not suspected previously in CdS, and in unexpectedly large amounts. In particular, appreciable amounts of the alkali and alkaline earth metals, including sodium, lithium, and calcium, were found in most of the Harshaw (G. E. raw material) and Eagle-Picher CdS crystal samples. A subsequent check for these materials by the emission spectrograph verified their presence in a wide variety of raw materials and crystal lots. It appears that most of the CdS lots have appreciable amounts of these impurities, and some lots have as much as 100 to 300 ppm of one or more of the alkali metal impurities. It is quite possible that 100 ppm of sodium, for instance, could completely mask the effects of a few ppm of certain other potentially electrically active impurities such as copper or silver.

The neutron activation analysis disclosed, and the mass spectrographic analysis verified, the almost complete absence of chlorine in the CdS crystals, including those lots that had been deliberately doped with $InCl_3$ during growth.

Additional impurities in CdS which very probably could influence the electrical properties are: oxygen and cadmium (stoichiometric excess.) Recent measurements have disclosed fairly large proportions of oxygen in normally processed CdS crystals. This oxygen has been detected as $SO_4^=$ in quantities up to 100 ppm. (Just how the oxygen is incorporated in the CdS lattice and hence its electrical effect is still not accurately known.) It appears that much of the sulfur-bound oxygen is in the raw material as received or enters the material from various processing steps, particularly the low temperature oven drying of the powder in air atmosphere for protracted periods of time. Alternate methods of processing such as vacuum oven drying and argon-vacuum sintering, have been successful in reducing the sulfur-bound oxygen content in the grown crystal to levels below the limits of detection. We do not, however, have any measure of the amount of cadmium-bound oxygen remaining in the crystals. This, plus the effect of other impurities apparently varies so widely that attempts to measure directly the effect of eliminating one impurity, such as the sulfur-bound oxygen, have not been successful.

It has been evident for some time that normal preparation of CdS single crystals by vapor phase growth in inert atmospheres (such as argon, helium, or nitrogen) results in non-stoichiometric crystals with strong excess of cadmium. This excess may manifest itself as sulfur vacancies rather than interstitial cadmium, however, the effect electrically is to give an equivalent high concentration of donor centers in the crystals. CdS crystals grown in inert atmospheres from the purest available powder without any deliberate impurity doping have shown indicated carrier concentrations in the range of 10^{17} to 10^{18} per cm^3. When the same materials are grown in an atmosphere of H_2S (or other sulfur bearing atmosphere,)the indicated carrier concentrations are in the range of 10^{14} or less, and the resistivities are increased from about 1 ohm-cm to the range of 10^5 to 10^9 ohm-cm.

It is apparent that we have yet to see really pure cadmium sulfide. The electrical properties of really pure CdS crystals remain unknown. It is possible that the extreme purification of CdS will result in hitherto unexpected and possibly useful electrical and/or optical properties. In any case, such material would be extremely valuable because it would make possible an accurate determination of the effect of various amounts of various impurities and crystal imperfections, and would permit more accurate tailoring of CdS material for specific physical, electrical and optical applications.

CRYSTAL GROWTH

Equipment

In June, 1961, The Harshaw Chemical Company, Solid State Research Department, moved to a new laboratory at 2240 Prospect Avenue, Cleveland. At this time the CdS vapor phase growth furnaces were torn down and completely rebuilt at the new location. Figure 1 is a photograph of the furnace layout at the new laboratory. The power facilities and temperature indicating and controlling equipment are mounted on a common power and control panel that can be seen at the right of the picture. The main feature of this arrangement is that the power and temperature measuring and controlling equipment are terminated in jacks on a switchboard type control panel. This permits complete flexibility for the power supplies, controllers and programmers of the three different furnaces. Thus, any of the power supplies or temperature controllers or indicators can be switched from one furnace to another by the insertion of a patch cord. This has given flexibility in the use of the equipment and has enabled three furnaces to do an equivalent number of growth runs previously done by four furnaces.

The furnace pictured at the left in Figure 1 is a small 2" diameter tube furnace for experimental runs, where larger ingots are not desired or required. The center furnace is a small 2" diameter high temperature tube furnace, constructed with an inner lining of K-30 furnace bricks, which can be operated at temperatures up to 1600°C.

The furnace on the right in Figure 1 is the large facility for "production" growth runs and large sintering-purification runs. This furnace takes a 3½" I.D. quartz tube and yields ingots weighing 700 to 800 grams each, or sinters of 2500 grams.

Growth Runs

During the period of performance of this contract most of the developmental and engineering efforts went into the evaporated CdS film cell. Because the film cell required less CdS material than the single crystal cell, and because purified sintered powder was used in the place of single crystal chips for most of the evaporated films, the requirements for single crystal CdS ingots were greatly reduced. Growth runs were made for evaluation of experimental variables

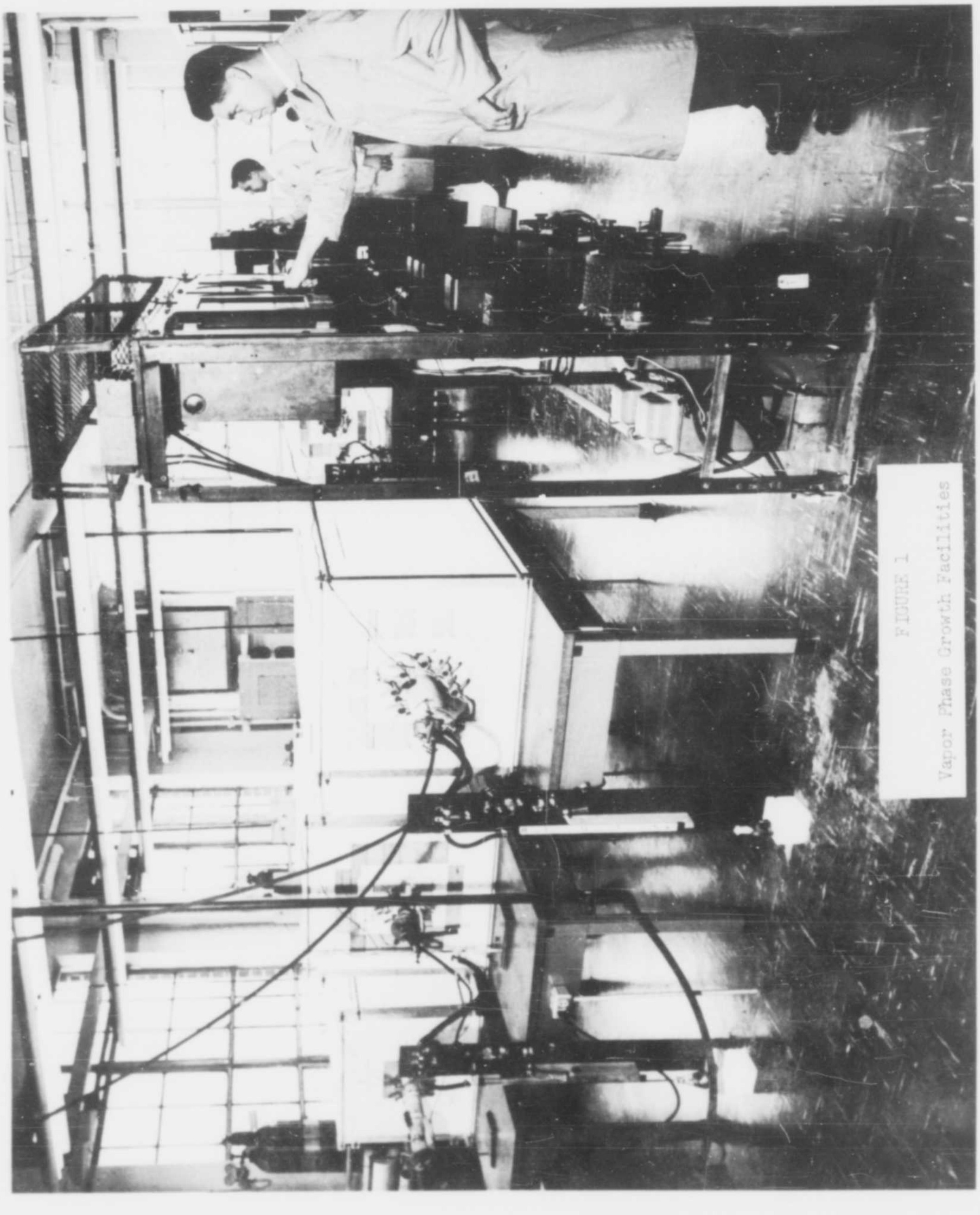

FIGURE 1

Vapor Phase Growth Facilities

(such as various dopants) and for some production of single crystal material for the supporting fundamental research studies. These studies did not require large quantities of single crystal material. Because of the shift in emphasis away from the CdS single crystal cell, there was a corresponding decrease in the amount of the experimental work pointed towards improving the techniques of single crystal growth.

A few studies have been made on the controlling temperature gradients in the vapor phase growth furnaces, on the growth of CdS under various atmospheres, and on the growth of CdS in a vacuum. Over the period of this contract a total of 36 single crystal growth runs were made in both the experimental and production type furnaces. The techniques employed for these were essentially the same as employed previously, and the results of the runs were comparable to those reported earlier.(2)

Vacuum Growth

Vapor phase growth of cadmium sulfide has in the past most successfully been carried out at temperatures in the range of 1250° to 1300°C. This has usually been done in inert atmospheres such as nitrogen, helium, or argon at approximately atmospheric pressure. The transport of vapors of CdS and/or cadmium and sulfur from the feedpile region to the cooler seedplates could be carried out at much lower temperatures if the ambient pressure were also reduced. There are potential advantages to growth in relative vacuums. CdS crystals with a reduced proportion of sulfur vacancies might result from the use of lower growth temperatures. The growth time might be greatly reduced, and there would be an economic advantage to not operating above the recrystallization temperature of the quartz tubes. A single quartz tube might thus be used for a number of runs rather than being expended for each run.

In an attempt to establish the conditions for vacuum growth, runs were made at various temperature conditions. For the first run, the temperature was reduced to just over 1,000°C at the feedpile and the seed plates were positioned at the normal locations for a regular 1250°C vapor phase growth run. However, no material was obtained on the seed plates. All the feedpile had sublimed and carried beyond the secondary seed plate onto the quartz wool plug or into the open end of the growth chamber beyond the quartz wool plug. A second vacuum growth run was made with the control temperature further reduced to 870°C. No primary ingot was established, but a very small secondary ingot did result which was microcrystalline.

A third growth run was made reducing the control temperature to 760°C. In this case both a primary and a secondary ingot were obtained. The primary ingot weighed 170 grams and the secondary ingot 173 grams. Both ingots were very microcrystalline in nature. This last growth run was a standard .003% $InCl_3$-doped run and the resulting material was reddish amber in color. From thermocouples positioned at the seed plates of this run, the temperature gradients were obtained. In general, the distribution of temperature in the growth tube was not as uniform as normally experienced during regular inert gas atmosphere growth runs. A larger than usual temperature gradient was experienced which probably resulted from the lack of a gas atmosphere inside the tube. Such atmosphere would help to equalize temperatures by a convection process. The ingots obtained from the vacuum growth runs were all hollow cup-shaped rather than solid cylindrical shaped as normally experienced. This indicates that the cooling pattern at the seed plate is appreciably different during a vacuum growth run than during inert atmosphere growth runs.

The absence of atmosphere reduces conduction of heat away from the seed plates. An attempt was made to increase this by placing a layer of steel wool behind and in contact with both primary and secondary seed plates. For this run the control temperature was increased to 800°C and held at temperature for 76 hours. In spite of the steel wool heat sinks, however, the ingots were still hollow cup-shaped and microcrystalline. Light amber colored 212 gram primary and 351 gram secondary ingots were obtained.

It appears that vacuum growth can be obtained at temperatures of 750 to 800°C, but that in this range the growth is very microcrystalline. From these studies, and from other considerations, it appears that the large single crystals obtained from the standard higher temperature vapor phase growth runs result from grain boundary migration(3) subsequent to nucleation. This grain boundary migration phenomena appears to be greatly temperature dependent and higher temperatures in the range of 1250 to 1300°C, are required to obtain grain sizes of several centimeters. Therefore the vacuum growth of CdS single crystals was not carried further.

H_2S Atmosphere Growth

From findings of elemental cadmium and sulfur in the cooler portions of the quartz tube during regular sinter-purification and vapor phase deposition runs, and from observations made during vacuum evaporation of CdS films it has become evident that there is appreciable dissociation of the CdS at the temperatures employed. When these high temperature operations are carried out in vacua or in inert atmospheres, the resulting CdS material apparently always has an excess of cadmium. Such crystals are characterized by low electrical resistivity. The resistance is generally in the range of 1 ohm-cm and Hall measurements disclose the crystals to be n-type with carrier concentrations of 10^{17} to 10^{18} per cm^3, even though no appreciable amount of donor impurities were deliberately added, nor as far as it is known accidentally included.

In an effort to eliminate the interstitial cadmium, or sulfur vacancies, in CdS crystals, a number of lots were grown using a sulfur atmosphere during crystal growth. The sulfur atmosphere was obtained by keeping an ambient of H_2S gas throughout the period of crystal growth and subsequent cooling to room temperature. A flow of H_2S gas was maintained to ensure sufficient sulfur excess in the ambient. Several such H_2S atmosphere growth runs were made using doped and undoped starting CdS material.

Growth in H_2S atmosphere appears to have been successful in practically eliminating the cadmium excess and/or sulfur vacancies which had previously been experienced. Of the several undoped lots grown by these techniques the resulting crystals had dark resistivities in the range of 10^7 to 10^{11} with little photoconductivity being exhibited. Crystals from the runs that were deliberately doped with other impurities exhibited resistivities in the expected range in each case. For these lots it is assumed that the excess cadmium has been compensated and that the conductivity is almost entirely due to the donor dopants deliberately added. Electrical and optical tests of these H_2S atmosphere grown crystals are not yet complete. It is expected that these studies will make possible the determination of the role of excess cadmium and/or sulfur vacancies in the formation of trapping levels, with consequent effect on the optical absorption spectrum and on cell spectral response. As far as can be determined, growing in H_2S makes no appreciable difference to the rate of crystal growth or to the ultimate crystallite size.

Homogeneity

Throughout our experience with the growth of cadmium sulfide crystals from the vapor phase there have been numerous indications of non-uniform distribution of both those impurities deliberately added and those residual impurities present in the starting material. Such a non-uniform distribution of impurities is to be expected since most impurities would have different vapor pressures than the cadmium sulfide at the temperature of crystal growth. (Appreciable differences have been noticed in this respect between different salts of the same cation impurity.)

Partially compensating this tendency for impurities to segregate because of differences in vapor pressure is a diffusion mechanism which should be very marked at the high temperatures and extended times of growth. However, the solid state thermal diffusion of impurities has obviously not been sufficient to counterbalance the effect of fractional distillation occurring during vapor phase deposition. Quantitative analyses of indium content in CdS ingots have disclosed variations as great as an order of magnitude between the two different ingots in one growth run, and variations of severalfold between the first and last portion of the ingot to grow. The amount of the feed pile material used during a growth run makes a big difference to the homogeneity of the impurities in the grown ingots. If all of the feed pile is sublimed during the growth process, all of the impurities that were present in the feedpile would also be sublimed and those with a lower vapor pressure than CdS would tend to concentrate during growth in the shrinking feed pile. Therefore they would tend to build up to a higher concentration in the last portion of the CdS ingot to grow, and vice versa.

A test was run to measure directly the variation in electrical properties of cadmium sulfide crystals due to impurity segregation. Two large single crystal grains, one from an $InCl_3$-doped lot and one from an undoped lot, were selected from suitable primary ingots. A rectangular parallelopiped extending from the seedplate position to the last portion of the ingot to grow was cut from each crystal. Successive slices, about 2 mm thick were then cut from each parallelopiped starting at the seedplate end, and the relative position of each slice was identified and this identity maintained throughout the subsequent measurements. Resistivity and room temperature Hall measurements were measured on each successive slice. Tables IV and V give the data obtained on the $InCl_3$-doped crystal and the undoped crystal respectively.

In Table IV it is seen that the resistivity varied from about .14 ohm-cm at the seed plate end of the ingot, to .06 ohm-cm at the top end of the ingot, while the number of carriers more than doubled. It is interesting that the resistivity and the number of carriers varied very little indeed (less than 10%) over the first half of the ingot to grow. Most of the variation occurred in the last half of the ingot to grow. The resistivity is decreasing as the ingot grows indicating that the $InCl_3$ dopant has a lower vapor pressure than the CdS at the temperature of crystal growth. Thus the indium tends to build up in the later portions of the crystal to grow when its concentration in the feedpile is greater.

In Table V, a greater variation in the electrical properties of the undoped material is evident. Here, over approximately the same distance from the seed plate to the last portion of the ingot to grow, the resistivity changed over several orders of magnitude from 2.4 ohm-cm at the seed plate, to 165 ohm-cm at the next to last slice, to a very high figure that we were unable to measure at the very last portion of the crystal to grow. The number of carriers decreased over this range by 2 orders of magnitude. It is to be noted that the resistivity change in the undoped material was in the opposite direction to that of the doped material, increasing as the crystal grew. This indicates only that on balance there was probably a decrease in donor type impurities as the crystal continued to grow. This change in resistivity must have occurred from a change in the distribution of the residual impurities in the raw material, which have previously been shown to be at or slightly below the limit of spectrographic measurements. It is probable that a moderate difference in the segregation of donor relative to acceptor impurities occurred here to cause a much larger order change in resistivity.

FILM CELLS

General

While many others have successfully vacuum evaporated films of CdS, and some have tried to fabricate photovoltaic cells from such vacuum evaporated films,(4) it was only recently that this has been accomplished with appreciable amounts of power output being obtained. This was accomplished on a separate Air Force sponsored research project(5) at The Harshaw Chemical Company early in 1960. The first CdS film cells were rear wall cells formed from vacuum evaporated CdS films laid down on conducting glass substrates. The areas were small, mostly less than a few square cm. The efficiencies were low, mostly less than 1%. It was very difficult to repeat results, and thus the

TABLE IV

ELECTRICAL MEASUREMENTS ON CONSECUTIVE SLICES OF .003% $InCl_3$ - DOPED CdS

(Samples from 1 Single Crystal Grain, Lot H-6, Cut Parallel to Seed Plate)

Distance of Slice from Seed Plate (mm)	Resistivity (Ohm-Cm)	Number of Carriers ($/cm^3$)	Hall Mobility (cm^2/volt-sec.)
1	0.141	1.27×10^{17}	348
4.4	0.146	1.25×10^{17}	344
7.8	0.14		
11.0	0.132	1.3×10^{17}	366
14.5	0.132	1.38×10^{17}	344
18.0	0.12		
21.2	0.109	1.54×10^{17}	374
24.6	0.08		
28.0	0.064	2.9×10^{17}	341

Note: Measurements taken in dark at room temperature. Readings remeasured and minor corrections made from data previously released in Third Quarterly Progress Report, this contract.

TABLE V

ELECTRICAL MEASUREMENTS ON CONSECUTIVE SLICES OF UNDOPED CdS

(Samples from 1 Single Crystal Grain, Lot H-7, Cut Parallel to Seed Plate)

Slice	Distance of Slice from Seed Plate (mm)	Resistivity (ohm-cm)	Number of Carriers (/cm^3)	Hall Mobility (cm^2/volt-sec.)
1	1.	2.43	6.54×10^{15}	393
2	4.4	3.87	$4. \times 10^{15}$	402
3	7.8	5.94	2.75×10^{15}	379
4	11.0	7.52	2.06×10^{15}	405
5	14.5	10.7	1.38×10^{15}	424
6	18.0	21.0	0.77×10^{15}	388
7	21.2	165.	0.096×10^{15}	395
8	24.6	Very high	(unable to measure)	

Note; Measurements taken in dark at room temperature. Readings remeasured and minor corrections made from data previously released in Third Quarterly Progress Report, this contract.

yield of such cells was very low indeed.

However, it was evident that film photovoltaic cells could be fabricated from vacuum evaporated CdS layers. There was promise that such cells could be fabricated much larger in area than single crystal cells, and that they would also be low in cost and might be capable of achieving high power to weight ratios.

Most of the attention of the present contract, which this report summarizes, was therefore devoted to the objectives of learning how to make CdS film photovoltaic cells in large areas, at higher conversion efficiencies, and to make these reproducibly and to achieve high ratios of power per unit of weight.

The initial work was carried on with back wall film cells on conducting glass substrates, but some attention was also given to alternate substrate materials. During the last 6 months attention was concentrated chiefly on front wall CdS film cells on substrates of molybdenum metal foil. The efficiency of the evaporated CdS back wall film cell gradually increased over this period from mostly less than 1% to as high as 4.95% on small area cells. During the last 6 months of the contract the efficiency of front wall film cells on molybdenum metal foil substrates has increased from mostly less than 0.5% to mostly between 0.5 and 1.0% for large areas of 9 in^2. Small area front wall cells have given efficiencies as high as 2.5%.

The processes for fabricating film cells show every indication of being reasonably economical in production, compared with those for making single crystal photovoltaic cells. Therefore, these advantages of large area, low cost and high power per unit of weight make the film CdS photovoltaic cell an extremely promising development.

Backwall Cell

Process

The method of fabricating back wall film cells is described in broad outline. Soda lime glass, such as is used for microscope slides, or pyrex glass is used for a substrate. The glass is cut to size (varying from 1" x 3", to 1½ x 3", or to as much as 3" x 3".) The thickness of the slides can be as little as .003 to .006", but usually is in the range of .040" to .062". The glass is first cleaned and then frosted on one surface in an HF frosting solution. Then a layer of conductive SnO_2 is applied to the frosted surface by the standard process of thermal decomposition of a $SnCl_4$ solution. This is carried out at a temperature of approximately 450 to 500°C. Successive layers of SnO_2 are applied in this fashion until the lateral resistance of the coating is below 30 ohms per square.

In order to reduce the sheet resistance further, and thus minimize the series resistance of the resulting CdS film cells, current collecting stripes are applied to the transparent conductive SnO_2 layer. These stripes may be of a fired silver-glass flux composition, or evaporated metallic silver or indium stripes. These are normally about 0.5 mm wide and spaced about 8 mm apart. They usually run the length of the glass slides. Best results were obtained with about 1000 Å thick evaporated indium stripes. The fired silver stripes tended to cause the evaporated CdS film to have poor structure where they overlapped. Also, the indium seemed to make better contact to the cadmium sulfide than the silver did. At the end of each slide, the collector stripes are joined by a heavier lateral stripe which acts as a collector bus.

The glass slide is then placed in the vacuum evaporation chamber, the pressure is reduced to about 10^{-4} Torr, and the slide is pre-heated to temperatures ranging from as low as 150°C to as much as 300°C. CdS is evaporated onto the SnO_2-coated surface at a rate of approximately 200 microns per hour. CdS single crystal chips, or CdS purified sintered powder has been used as the source of material, in either doped or undoped form. Special conically shaped evaporation boats are employed to hold the material during evaporation. A perforated lid shield covering the mouth of the boats is used to prevent large particles of CdS from being thrown up onto the glass slide. Heavy CdS films, .0015 to .003" thick, have been found necessary for continuity and in order to secure satisfactory I-V characteristic curves of the subsequent cells.

The lateral resistivity of the evaporated CdS films has been found to be in the same range as the single crystals used for starting material, or of single crystals grown from the vapor phase from the same sintered powder starting material. The carrier concentrations of the evaporated films have also been in the same range as those of the single crystal material, though the Hall mobility measured laterally is normally 1 to 2 orders of magnitude lower than that of corresponding single crystals.

Barriers are formed on the CdS films by electroplating finely divided copper and heating in the presence of air. The procedure is identical to that used in forming barriers on CdS single crystal slabs. Contact is made to the barrier by applying an air drying conductive silver paint. Figure 2 illustrates the construction of a typical back wall CdS film cell on a conductive glass substrate. Cell illumination is through the glass substrate and SnO_2 layer and through the CdS layer to the barrier region. Hence the name "back wall" cell. The negative electrode of such a cell is the SnO_2 coating, while the positive electrode is the silver paint which has been applied to the barrier surface.

Performance

Initially only very small portions of evaporated CdS films could be successfully used for fabricating into photovoltaic cells. Most of the film areas gave a low resistance ohmic contact from the conductive SnO_2 layer through to the silver print, instead of a rectifying barrier. A number of factors were found to be causing this situation and these were gradually recognized and corrective actions were taken. Some of these factors were:

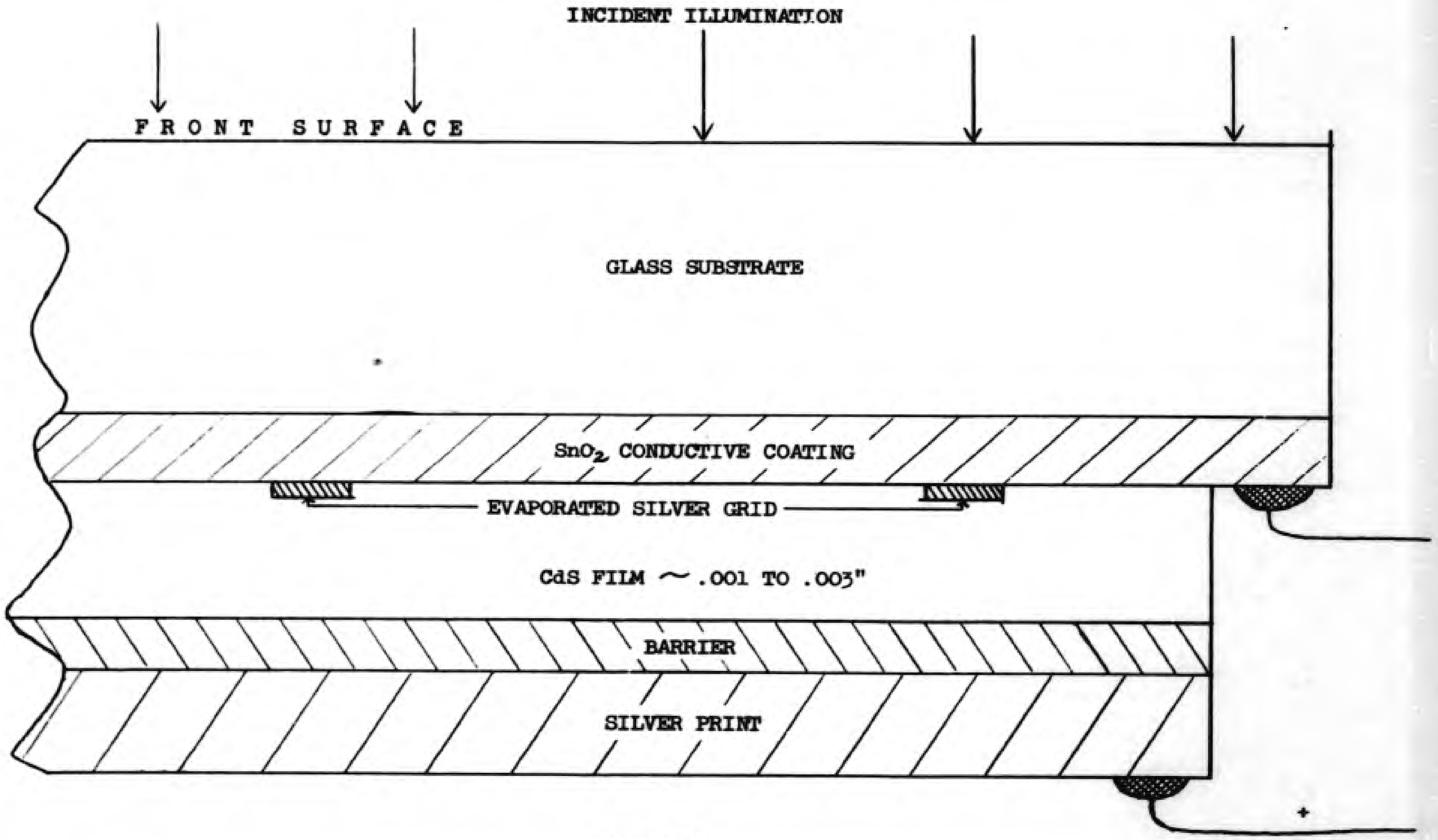

FIGURE 2

Enlarged View of Backwall CdS Film Cell Showing Construction too much antimony dopant in the tin oxide coating, pin holes in the evaporated CdS layer due to flaws or soil on the substrate, poor CdS film structure due to too low a temperature of the substrate during evaporation, and too thin a CdS film.

This latter factor has been found to be very important indeed for the CdS film photovoltaic cells. When a number of back wall film cells were made for reproducibility studies, it was found that there was a direct correlation between the average film thickness and the cell efficiency. With films less than about .001" thick only very low efficiencies (under 1%) could be obtained. As the film thickness was increased to .002" and .003", and even up to .005", the cell efficiency gradually increased until it tended to approach that obtained on single crystal cells (4 to 5% on small areas.)

Lightweight Cell

The active portion of the CdS cell, the barrier region, is apparently very thin - probably less than a micron. The bulk n-type portion can also be thin - about .001" to .002" for the evaporated film cell. The substrate itself needs to be only thick enough to hold the cell together physically. Therefore, a reasonable basis exists for obtaining a truly thin light weight cell that might have an appreciably higher power to weight ratio than obtainable from other, higher efficiency, single crystal cells.

The glass substrate comprises the major part of the weight of the CdS film cell. Therefore, a number of possible substrates were considered and evaluated for a light weight cell. An attempt was made to evaporate CdS films on these various possible substrates. Thin "Mylar" and "Tedlar" plastics, mica, ribbon glass, glass paper and various glass-plastic laminates and fabrics were considered and tested. Table VI summarizes the experience with these materials when CdS films were evaporated on them.

Of the materials tested, the teflon film-glass paper laminate seemed to produce the most satisfactory film in regards to porosity. However, a number of pinholes were still evident even though the films were 50 microns thick.

Several preliminary attempts were made to form a transparent conductive electrode at relatively low temperatures on the teflon filled glass paper substrates. [Glass paper can be made conductive by a higher temperature pyrolysis technique in the manner disclosed by M. Jaffe(6), but these suffer from the tremendous disadvantage that they are very fragile. Also they are so porous that we have been unable to form non-porous CdS films on such substrates.] When 100 Å of Bi_2O_3 and 100 Å of Au were evaporated onto the teflon filled glass paper laminate and heat treated for 5 minutes at 300°C after the manner disclosed by Ennos,(7) a sheet resistivity of 90,000 ohm/sq. resulted with an optical transmission of only 20%. When 300 Å of PbO and 200 Å of Au were evaporated on this material and heated for 2 minutes at 200°C, a sheet resistivity of 5-10 ohm/sq. was obtained. The transmission was still

TABLE VI

PRELIMINARY EVALUATION OF VARIOUS POSSIBLE LIGHT WEIGHT SUBSTRATES FOR EVAPORATED CdS FILMS

Substrate	Comment
Mylar	Apparently decomposed by heat radiation from filament. Might be successful if placed at greater distance from filament.
Teflon	Film formed. Thermal expansion coefficient mismatch caused curling and cracking of film. Might work with thinner teflon or thinner CdS film.
Mica	Bad thermal expansion coefficient mismatch caused severe curling and peeling. Completely unsatisfactory.
Ribbon Glass	Thermal expansion coefficient mismatch caused peeling.
Glass Paper	Film formed, but did not bridge holes in mat that were larger than about 0.1 mm in diameter.
Teflon-Glass Paper Laminate	Film formed, but porous character of substrate carried through to CdS film. Some curling with radius of about 5 cm.
Woven Glass Fabric	Extremely porous film formed.

only 20%, but this might be improved since in this case there was a very poor optical coupling between the film and the detector cells for the transmission measurement.

The teflon-glass paper substrate may still be a practical substrate for a light weight CdS film cell, but a great deal of further development work might be required before this could be realized.

Attempts were made to form an SnO_2 film on .002" thick ribbon glass substrates by standard pyrolysis techniques. In each case the glass ribbon would not withstand the temperature required. Apparently the glass ribbon is under a great deal of stress and when the temperature is increased to the range of 400°C the surface tension of the glass causes it to curl into very small globules.

From the experience with the above materials, it has become apparent that in order to secure a very thin cell, the thermal coefficient of expansion of the substrate must closely match that of the cadmium sulfide itself. Otherwise when the temperature changes, the film and the substrate will expand or contract at different rates, causing extreme curling, and possibly peeling. (Considerable mismatch might be feasible if the substrate were rigid enough to resist curling, but this does not seem possible in a very light weight cell.) It is necessary that the films be able to withstand appreciable temperature variation since they must be formed at several hundred degrees centigrade. The thermal expansion coefficient of CdS is approximately $5 \times 10^{-6}/^{o}C$. There are glasses and metals that can be found in this range but there is apparently no plastic that fits the requirements.

Consequently we are limited to either a thin conductive glass or a metal foil such as tantalum or molybdenum. A very thin SnO_2-coated microsheet glass in the range of 30-50 ohms/sq. resistance, was obtained from the Corning Glass Works. This glass was .0025" thick. A number of attempts were made to evaporate CdS films on these substrates and to process these into photovoltaic cells. In a few instances such films were vacuum evaporated successfully. This glass is under extreme stress, possibly from the SnO_2 coating, and any normal handling caused them to shatter. In a number of attempts to process such films into cells, a few small area cells were successfully fabricated, but in no case could a cell as large as 1 x 3" in area be carried completely through the process without breaking of the substrate.

Molybdenum and tantalum metal can be readily obtained in thicknesses to .0003" to .0005". However, these metals are opaque to the wavelengths required for solar cell operation. Therefore with these metals we are limited to front wall cell operation.

Molybdenum and tantalum have both been evaluated for the purpose. The molybdenum metal foil has been more successful because it is more readily cleaned and etched. Hence, reasonably good CdS film adhesion is obtained. The work with the front wall molybdenum substrate cell is described in the following section.

There is one possibility of using a metal foil substrate and still having a back wall cell. This is to use a perforated form of the metal and to shine the light through the perforations to the film beyond. To check this possibility, a special molybdenum screen was purchased. The screen was 25 microns thick and contained closely spaced 150 micron diameter holes with a total of 62% of the metal area removed. The screen was backed up with a sheet of mica and a film of CdS was evaporated onto the combination. A photovoltaic cell was processed from this film and illuminated through the substrate as a back wall cell. The cell had an open circuit voltage of 0.5 volts and a short circuit current density of 4 ma/cm^2. The conversion efficiency was only 1.0%. This approach has possibilities, but a lot of further work will be needed to achieve practical cells with high power outputs per unit of weight. At the present time, the front wall cell on solid molybdenum foil substrates looks more promising.

Front Wall Cell

Front Vs. Back Wall Operation

The sheet resistance of the very thin "p-layer" of the CdS barrier surface is a major problem that may be the reason that higher efficiencies have not been obtained when the cells are used as front wall devices by illuminating the barrier directly. This difficulty has been at least partially circumvented by the application of a grid electrode to the surface of the barrier, similar to the technique used to reduce the sheet resistance of silicon solar cells. These grid electrodes sacrifice a portion of the active area of the cell by blocking the light from the area they cover. However, there is an advantage to front wall operation which partially offsets this sacrifice of active area. This is an enlarged spectral response, due to the conversion of wavelengths of light shorter than the absorption cutoff of CdS. The enlarged spectral response can be seen in Figure 3. A CdS cell on a glass substrate was used for this measurement with one half of the cell finished as a back wall cell and the other half finished as a front wall cell. Less output was obtained from the front wall cell, but the response was extended into the near ultraviolet region of the spectrum. The conversion efficiency of the back wall portion of the cell was 1.5% and only 0.4% for the front wall portion. However, when the front wall portion was covered with silver print and illuminated as a back wall cell, it also gave 1.5% conversion efficiency. Therefore, the problem of realizing higher efficiency from the front wall cell appears to be primarily that of the sheet resistance of the p-region, i.e. it is a problem of collecting the current from the barrier.

However, the sheet resistance may not account for the entire difference between the front wall and the back wall cell outputs in this instance. It is possible that there is a thin film of Cu_2O or other material on the barrier which does not contribute to the operation of the cell and yet which acts as a gray filter to remove a proportion of the light which would otherwise reach

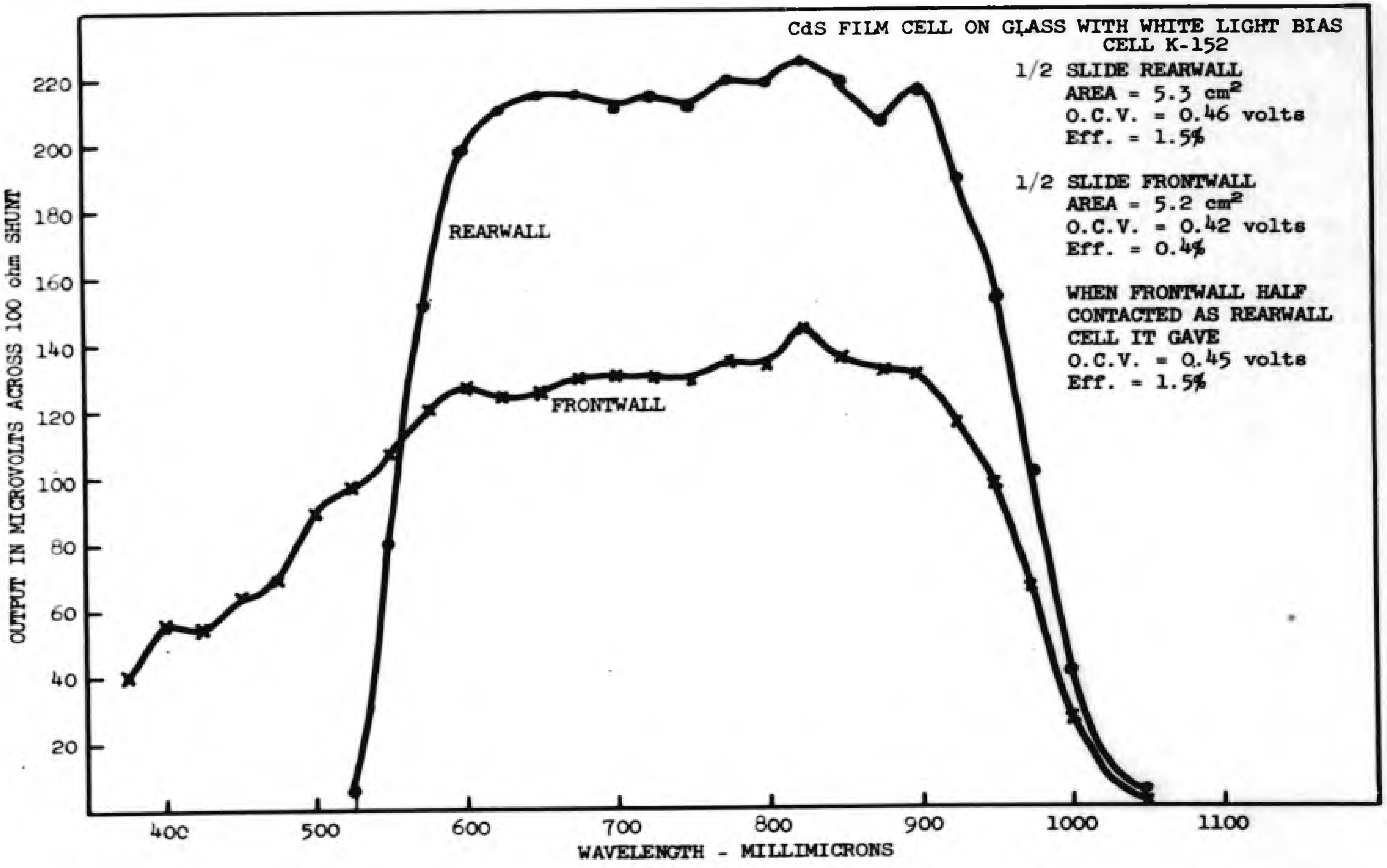

FIGURE 3

Backwall vs Frontwall Spectral Response

the barrier. Some attempts have been made to remove this presumed Cu_2O layer but without complete success.

Process

The process for evaporating cadmium sulfide films on molybdenum substrates is very similar to that for evaporating cadmium sulfide on glass substrates, except that the methods of preparing the substrates are different. In particular, a molybdenum surface must be thoroughly degreased and then etched to provide a roughened surface to secure adhesion of the CdS film. This has been done by strongly oxidizing the surface of the molybdenum in a 1:1 HNO_3 bath followed by a conc. HCl rinse to remove the oxide layer.

Other variations in the process were necessary to cope with the very thin substrates. The substrate heater (for the vacuum evaporation operation) had to be changed from a conduction type heater to a radiation type of heater in order to secure reasonably even heating of the substrates. Extreme care had to be exercised in the manner in which the substrate was clamped into the substrate holder. The method of clamping the very thin substrates into the substrate holder had to be carefully engineered to prevent the substrate holder from becoming a heat sink and giving rise to temperature gradients across the substrate which would adversely effect the film deposition. Also, the adhesion of the CdS films to the molybdenum seems to be sensitive to variations in the structure of the molybdenum itself.

Initially, .005" thick molybdenum metal was used as substrate material and a tentative process for fabricating front wall CdS evaporated cells on such substrates was evolved. These cells had conversion efficiencies up to 1%, but were extremely variable in output. (Subsequently, the thickness of the molybdenum was reduced to .002" and then to .001".) A pilot production line was set up and an attempt was made to fabricate such front wall CdS cells reproducibly. A number of problems in the processing, chiefly centering around the vacuum evaporation of the CdS film itself, soon became evident and were largely brought under control. The more important of these problems were the uniformity and thickness of the CdS film, and the continuity of the films. These problems were solved largely by careful tooling and engineering of the evaporation setup.

Operation of the pilot line was of considerable assistance in defining the problems involved in front wall film cell operation and in evaluating some of the major variables. The better cells obtained from the pilot line operation were used to work out the process of laminating film cells into arrays.

Performance

More than 250 CdS front wall film cells, each 1" x 3" in nominal area, have been fabricated on .002" thick molybdenum foil substrates. The efficiency of these cells varied between 0 and 1.0%. After the process was brought under a reasonable degree of control, the efficiencies varied mostly between 0.5 and 1.0%. At this point we found it practical to increase the area of the cell to 3" x 3". The efficiency stayed approximately the same. About 85 of these cells were made, mostly for the larger area arrays, and their average efficiency was 0.6%. These cell efficiencies are calculated on the basis of the total barrier surface area rather than on the area exposed to the light. Thus, the actual efficiency of the active, or actually exposed area, would be approximately 20-25% greater.

During the operation of the pilot line some observations have been made which are pertinent to the problem of increased cell output. In nearly all instances films thinner than about .0007" yield cells that are resistors rather than rectifiers. As the evaporated film thickness increases, a better rectification curve is obtained and more output is obtained from the cell. Figure 4 illustrates the experience with cell thickness. Figure 4a shows the I-V characteristic curve of a typical film cell made from a very thin CdS evaporated film (approximately .0005".) The characteristic curve is a straight line through the origin with a very steep slope. In effect the cell is a low resistance short circuit and the same characteristic curve results under sunlight illumination as is obtained in the dark. As the film thickness is increased the characteristic curve increases in slope so that the resistor is a higher resistance resistor, and the cell acquires some photovoltaic output as illustrated in curve 4b. This curve is typical of cells obtained from films in the range of about .0007" to .0009". Curves 4c, 4d and 4e represent the I-V characteristic as the film thickness is increased further. It is seen that gradually a rectification curve results and the curve gradually acquires a rectangular characteristic when the film thickness approaches .002". At this point (figure 4e) the light curve acquires a desirable, nearly rectangular, I-V characteristic shape.

Another important point is that the substrate temperature must be maintained above approximately 250°C, or very poor cells result. Several effects may be involved here. Poor adhesion of the CdS to the molybdenum substrate is obtained if lower temperatures are used. This causes the film to peel from the molybdenum in severe cases, and in less severe cases results in poor barriers due to non-uniform plating current distribution and hence non-uniform deposition of the mossy copper layer during barrier electroding. Also, cooler substrate temperatures apparently permit too much free cadmium to be condensed along with the CdS giving a very heavy stoichiometric excess of cations. In these cases, the resulting semi-conducting layer appears to be degenerate and hence poor junctions are obtained. Other effects such as restricted grain growth due to the lower temperature may also be present, though verification of this effect is presently lacking.

It appears that a very high degree of dissociation of the CdS occurs during the evaporation process. It has been found that if very slow evaporation rates are maintained very little CdS is formed on the substrate. Apparently a relatively high partial pressure of both Cd and S vapors in the region of the substrate are required in order to form sufficiently thick films to yield

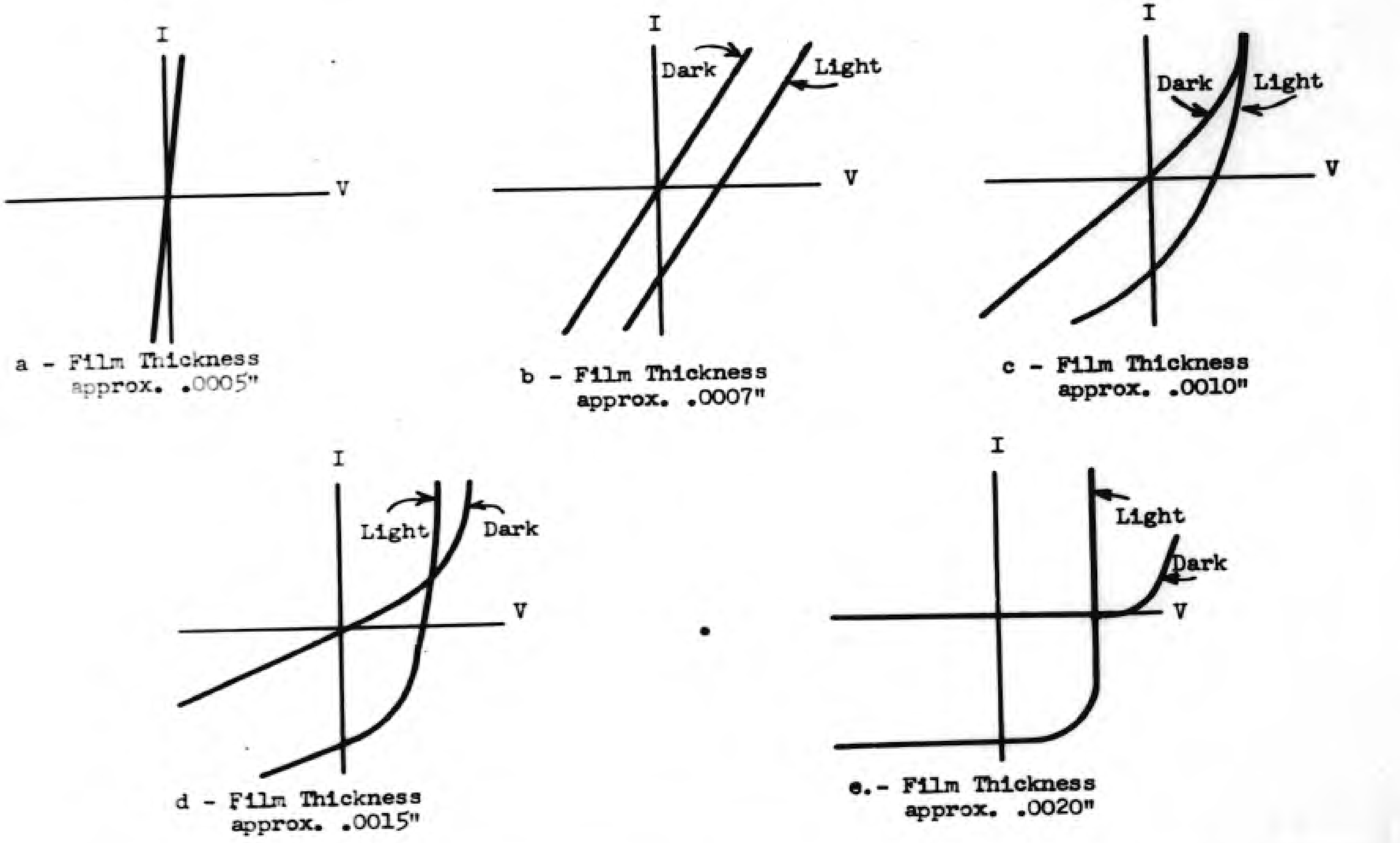

a - Film Thickness approx. .0005"

b - Film Thickness approx. .0007"

c - Film Thickness approx. .0010"

d - Film Thickness approx. .0015"

e.- Film Thickness approx. .0020"

FIGURE 4
Effect of CdS Film Thickness on Light and Dark I-V Characteristic Curves

good cells.

With a material such as CdS, which sublimes directly rather than melting and then evaporating, a problem of heating the material gradually to the sublimation temperature exists. When heating is done by conduction from the boat to the adjacent contacting CdS particles and/or by radiation from the boat to the outer surfaces of the adjacent CdS particles, there is danger of over heating some particles of CdS locally. This causes vaporization of some CdS with explosive violence. This is particularly the case when a high rate of evaporation is desired and when relatively small particles of CdS are used for the charge. The result is that many small particles of CdS are ejected from the boat as particles without vaporizing. Many of these particles reach the substrate and stick there (at least temporarily). This effect we have called "splattering". The result of splattering is poor structure of the resultant film. In a proportion of the cases the splattered particle may subsequently come loose (frequently in the strong HNO_3 barrier plating bath) leaving a hole in the film causing a short circuit in the finished cell. This problem has been alleviated by a combination of several factors including: the use of perforated "baffles" inserted into the mouth of each evaporation boat, an increase in the substrate to filament distance, and the use of special design evaporation boats such as the Kemet Company SiO evaporation source. (As obtained from Allen-Jones, Inc., Long Beach, California.) However, the problem is not completely solved and further work on this is planned. It is possible that heating the charge by induction heating may be the answer to this difficulty.

Cell Size

Most of the work on the front wall film cells on molybdenum substrates was done in either the 1 x 3" or 3 x 3" nominal size. This represents in each case the active area of the cell. It has been found that larger area films can be cut into smaller sizes using a paper cutter or sheet metal shear, or even ordinary household scissors. In this operation there is normally little or no flaking of the CdS film from the molybdenum substrate. It has also been found that finished cells can be cut into smaller pieces by the same method without any apparent damage to the barrier. In several cases, larger area film cells have been carefully tested prior to and after cutting into two or more smaller cells in this fashion. In each case, the sum of the power outputs of the smaller cells was equal to the power output of the larger area cells from which they were cut. No additional heating or other treatment was found necessary. Apparently the barriers of CdS film cells are much more durable than those of single crystal cells. This is possibly due to their polycrystalline nature and it may be that very small crystallites of the film cells are damaged by the cutting process but are not noticed in the overall effect due to the small portion of the total area which they represent. In a few cases, the cutting of the film cells into smaller areas does cause some of the silver print grid electrode to flake off from the cells. In such cases the grid can be readily re-applied. This feature of the evaporated film CdS cell opens interesting possibilities for economical production of such cells.

Surface Preparation

When processing single crystal CdS photovoltaic cells, it was found that in order to optimize the output from such cells the crystal surface on which the barrier was to be formed had to be "disturbed". A freshly cleaved crystal surface, or a crystal that had been annealed, or one that was deeply etched on its major surface prior to barrier electroding usually gave less than half the conversion efficiency that would be obtained from the same crystals where the barrier surface was disturbed prior to barrier electroding. Among various methods of disturbing the crystal surface, lapping with a coarse abrasive grit, such as Al_2O_3, on a cast iron lap was found to be as effective as any method tested.

Preliminary evaluation of such a technique on evaporated film cells has shown some indication that a similar process will help these cells. In several instances where controlled experiments were run, those films that were being disturbed by lapping with an abrasive grit prior to barrier electroding gave equal or better results than those that were not so treated. It appears that this technique may succeed in eliminating the lower efficiency cells but that it may not increase the upper limit of the conversion efficiency frequency distribution.

Why a disturbed CdS surface crystal should yield higher efficiency cells is not known. A possible explanation is suggested by the work of Rindner and Lavine(8) on the scribe plating of semiconductor surfaces. Lapping or other disturbance of the CdS surface could cause preferential nucleation sites for the copper during barrier electroplating, thus yielding a more microcrystalline deposit and eventually result in more activation centers at the barrier surface.

Multiple Evaporation

At the time when considerable difficulty was encountered with very thin films, a few attempts were made to re-evaporate a second layer of CdS in order to build-up the films to the desired .002" thickness level. In a number of these cases very encouraging results were obtained. Some very excellent open circuit voltages resulted that were approximately 10 to 15% higher than those obtained with singly evaporated films of comparable total thickness. Also, some of the highest efficiencies obtained from front wall cells were measured on cells that were made from doubly evaporated films. However, there were some difficulties also with this technique. Films that had been removed from the evaporator, measured for thickness, and then placed back in the evaporator frequently showed poor adhesion of the second layer. This may have been due to some kind of contamination or some adsorbed gas layer. The poor adhesion usually manifested itself by the second layer peeling during the barrier plating operation.

However, the method seems to offer real advantages if a degree of control can be exercised over these extraneous factors. Multiple evaporation might give a thinner overall film that would not exhibit shorting of the barrier through to the substrate, such as is obtained from a singly evaporated thin film. Several variations of this method of multiple evaporation have been made, but as yet the necessary structure studies have not been completed. It is believed that a re-nucleation occurs on the second and subsequent evaporations rather than epitaxial growth on the previously laid down crystal grains. If this is the case, it is probable that the grain boundaries from one layer do not normally coincide with those of the next layer. If so, the problem of shorting should be minimized, and much thinner films might be utilized with a consequent decrease in the weight of the film cells and an increase in their flexibility.

ARRAYS

Design and Equipment

For usable devices the film cells must be connected together electrically, held facing the incident radiation, and protected from deleterious environmental effects. One practical approach to this is to encapsulate the cells and leads in a suitable plastic envelope. Such envelopes can be made very thin.

To perform this operation a laminating die was constructed consisting of two parts. The lower portion is a chamber which can be evacuated and which is topped by a flat porous metal plate. The upper portion is a chamber which is connected to a supply of compressed gas. In practice the cells to be laminated are placed with suitable series-parallel connections and external lead tabs in position between two sheets of clear thermoplastic on top of the porous metal plate. Sheets of release plastic are placed above and below the layout to prevent adhesion of the plastic to the porous metal plate beneath or to a thin sheet of aluminum metal foil which is placed above to act as a membrane between the vacuum and pressure chambers of the die during lamination. A seal is effected between the upper and lower portions of the die with a silicone rubber O-ring gasket, and the die is placed between the heated platens of a hydraulic press. The lower portion of the die is evacuated and the upper portion is connected to the compressed gas (usually nitrogen). Then the laid out array is pressed by the aluminum foil membrane against the porous metal plate. Air is evacuated from the layout through the porous metal plate, while the membrane presses the various layers of the array against the porous metal plate and the heat fuses the upper and lower sheets of thermoplastic to each other and to the film cells in between. At the same time, the leads and connecting tabs are held in place by the plastic until the conductive epoxy resin cement cures. Figure 5 shows the relative (not to scale) positions in cross section view of the components of the layout in the die just prior to the actual lamination. During lamination the plastic flows in between the cells and fills all of the cavities between the cells and lead tabs.

The actual schedule for the lamination process will vary somewhat with the thickness and type of plastic materials employed. A typical time-temperature schedule for lamination is illustrated by the use of high density polyethylene films of .002" thickness. After the layout is placed in the die, the die is

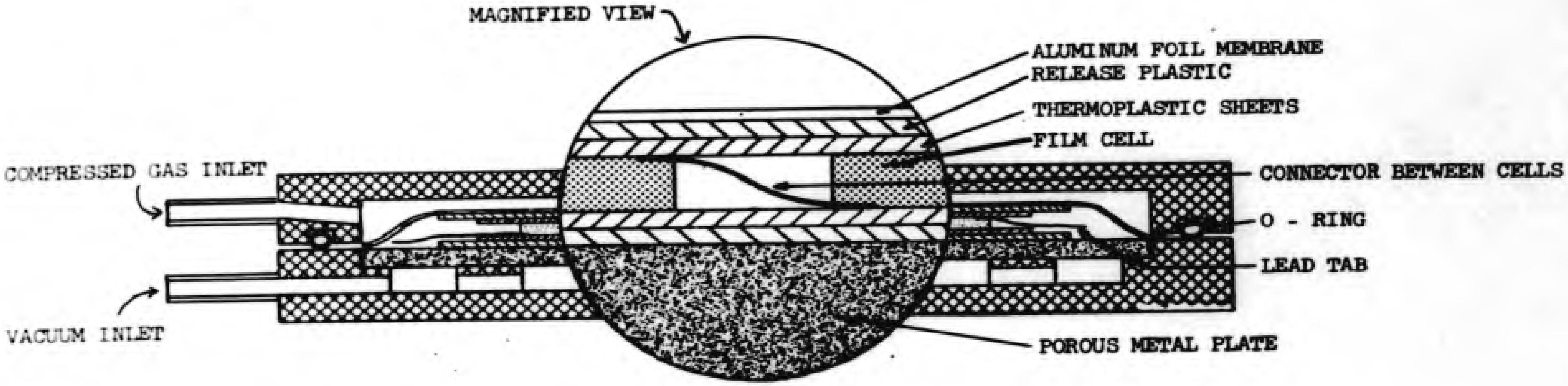

FIGURE 5

Layout of Array in Laminating Die Prior to Lamination placed between the heated hydraulic press platens at 400°F and the evacuation of the lower chamber is started. After one minute compressed gas at a pressure of about 100 psi is fed to the upper chamber and held for the next 2 minutes. The vacuum is held on the lower chamber throughout this period. During this time the platens are cooling slightly due to heat conduction into the die. Then, the upper and lower chambers are brought to atmospheric pressure and the laminating die is allowed to cool in place prior to opening the die and removing the laminated cell.

Materials

It is possible to laminate film cells between a number of thermoplastic materials. The choice of the plastic depends upon the physical requirements of the envelope as well as their compatibility with the CdS photovoltaic cells and the ease of fabricating them into an array. A number of thermoplastic materials have been initially evaluated as CdS film cell encapsulating materials.

High density polyethylene in .002 and .005" thick films were tested first. With this plastic .0005" mylar film was used as release plastic and a laminating temperature of 400°F was used for a time of 3½ minutes. The polyethylene formed a tight transparent envelope around the cells and leads and adhered well to the barrier surface. The cells retained their electrical and optical characteristics throughout the laminating process. There are some indications, however, that the polyethylene material does not form a moisture proof envelope and allows the cells to deteriorate in room atmosphere storage.

Trifluorochloroethylene (Kel-F) has been used in thicknesses of .005" and .001". With this material teflon-filled glass paper or Teflon film is used as release layer. The lamination was carried out at temperatures of 430°F for 3½ minutes. The Kel-F plastic gave some difficulty in not adhering well to the film cells. This difficulty was obviated by inserting a very thin (.00075") nylon layer between the cells and the Kel-F. The Kel-F seems to yield a laminate which is more resistant to moisture penetration under ordinary atmospheric storage conditions than the polyethylene.

Polyvinyl Fluoride (Tedlar) is a newly developed film material from duPont which is supposed to combine the heat stability of Kel-F with improved adhesion properties. This material was tried in .002" thicknesses using the same lamination schedule used for the Kel-F films. The Tedlar films did show some shrinkage in lamination but good appearing laminates were produced. The adhesion of the plastic to the cells was excellent and this material also seemed to be reasonably compatible with the CdS film cell barriers.

Polycarbonate (Lexan) is a highly temperature resistant film developed by General Electric Company. Temperatures of about 435°F were necessary in order to fuse the films. However, at this temperature the film deteriorates locally and forms small gas bubbles in and between the two layers of film.

A number of tests all yielded arrays showing these bubble defects and therefore this material was abandoned.

Polyester (Mylar) - Polyethylene composite films were employed to laminate CdS film cells. The samples tried consisted of .001" mylar film coated with .002" polyethylene films and were obtained from the Dobeckmun Company. Successful laminations were carried out using the same lamination schedule employed for polyethylene. The laminates were of good appearance and the material seemed to offer interesting prospects in combining the strength of mylar with the thermoplasticity of polyethylene.

There are, of course, a number of other requirements for the plastic envelope material other than adhesion, transparency and ease of lamination. Also important to varying degrees, depending upon the particular application, are permeability to oxygen and water vapor, compatibility with the CdS barrier, resistance to Van Allen radiation, temperature resistance, and the weight of film required for ruggedness and durability. A more complete evaluation of the various plastic materials mentioned above, as well as others that may still be acquired, is needed before a final selection can be made.

Results

In the closing months of the contract period nearly 100 laminated arrays have been constructed along the lines discussed in the previous sections. These arrays have been constructed from both 1" x 3" and 3 x 3" front wall film cells on molybdenum substrates. These various laminations have been carried out in order to work out the process of lamination and to study the performance characteristics of the laminated cells and their stability when laminated in various plastic materials.

A number of arrays of 36 sq. in. of active area have been constructed, these have usually been made of 4 individual 3 x 3" cells connected in series and laminated between sheets of various plastics. Typical of such arrays is the data of array No. 65 which was delivered to the Contract Monitor in November. This array was constructed with .004" Kel-F for the front surface. Beneath this layer was.00075" of nylon plastic for adhesion purposes. These were next to the cells which were .0015 to .002" thick CdS films on .002" molybdenum foil substrates. The lower plastic layer was .0015" Kel-F. The leads and tabs consisted of .001" thick silver foil ribbons approximately 1/8" wide and these were cemented to the cells with "Eccobond" 56C conductive epoxy resin.

Laminate No. 65 under one sun equivalent illumination (100 mw/cm^2 intensity) gave 1.65 volts open circuit, 160 ma short circuit current and a maximum power output of 100 mw. The conversion efficiency of the entire array was 0.5%. The active area of the 4 cells comprising the array was 213 cm^2 (including the collector grid pattern). The entire array weighed 22.5 grams giving a power to weight ratio of 2.3 watts per lb. Assuming that under extraterrestrial sunlight the open circuit voltage would remain the same and the short circuit and the maximum power output would be increased proportionately to the energy of the radiation (140 mw/cm^2), the extra-terrestrial sunlight power to weight ratio calculates to 3.2 watts per lb.

A number of other arrays of equivalent size were made with the individual cell conversion efficiencies as high as 0.9%. In most of these larger size arrays no particular attempt was made to minimize the weight of the arrays.

Some of these arrays can be seen in the photograph of Figure 6 clustered around a larger 1 square foot film cell array. The 1 square foot array was constructed of 4 smaller 6 x 6" arrays that were connected in series, heat sealed together, and then tacked to a backing sheet of .005" Kel-F plastic.

The performance of the 1 square foot film cell array was measured under simulated sunlight of 100 mw/cm^2 intensity. The open circuit voltage was 6.2 volts, the short circuit current was 136 ma., and the maximum power output calculated from the I-V characteristic curve at 415 mw for an efficiency of 0.5%. The active area was 870 cm^2 (or 135 in^2).

No attempt was made to reach a high power to weight ratio on this array. The array weighed 156 grams representing 1.25 watts per pound under terrestrial sunlight and 1.69 watts per pound under extra-terrestrial sunlight.

On one smaller area array an attempt was made to maximize the power to weight ratio. This was laminate No. 55 which consisted of a single 3" x 3" front wall cell on .001" thick molybdenum foil. This laminate was constructed with .001" Kel-F plastic for both front and rear surfaces with .00075" nylon plastic between the front Kel-F layer and the CdS cell. The rest of the construction was the same as for the 6 x 6" arrays described above.

Under one equivalent sun (100 mw/cm^2 radiation intensity) this array gave 0.45 volts open circuit, 220 ma short circuit current, for a maximum power output of 45 mw. This represents a conversion efficiency of 0.9%. The total area of this cell was 50 cm^2 and its overall weight was 2.91 grams. This represents a power to weight ratio of 7 watts/lb. under terrestrial sunlight and a calculated power to weight ratio of 10.0 watts/lb. under extra-terrestrial sunlight. This array was also delivered to the contract monitor, however, it degraded somewhat after initial testing and prior to such delivery. The .001" Kel-F plastic is obviously inadequate protection for such cells under ordinary atmospheric storage.

It is noted that this power to weight ratio was obtained from a cell of less than 1% conversion efficiency. There is reason to believe that improvements in power output are possible and will probably be obtained with further developmental efforts. Also, the weight of such arrays can probably be further reduced. Thus, without any further technological breakthrough, power to weight ratios in the range of 20 to 30 watts/lb. seem indicated. However, a great deal of further work is required before this objective can be realized.

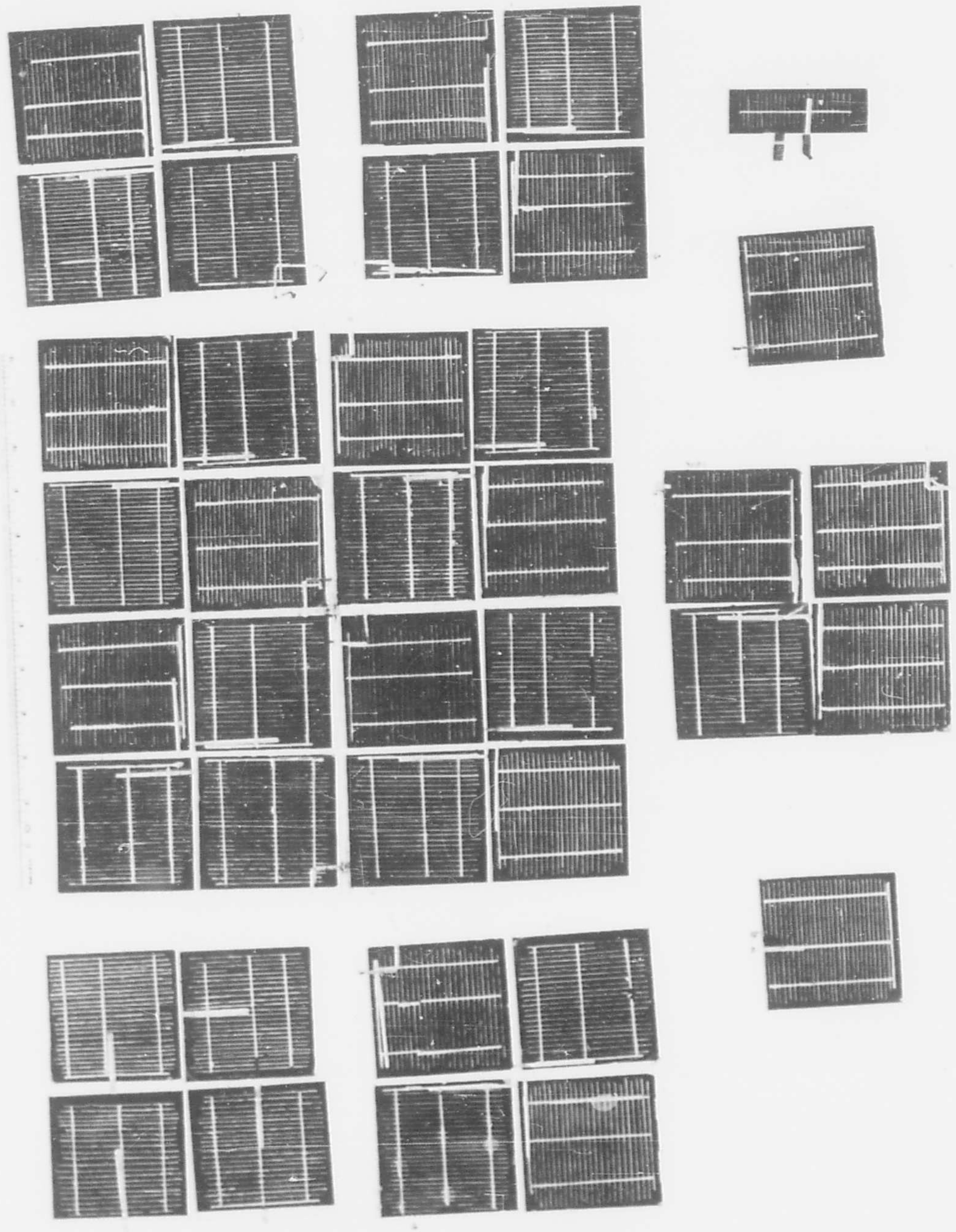

FIGURE 6
1 Square Foot CdS Film Cell Array and Several
6" x 6" Arrays, 3" x 3" Arrays and 1 - 1" x 3" Array

TEST DATA

Temperature

A typical I-V characteristic curve of a back wall CdS film cell on a glass substrate is presented in Figure 7. This cell had an area of about 5 cm^2 and, as can be seen from the curve, a rather high series resistance. This was because the particular cell did not have current collecting stripes and hence the sheet resistance of the SnO_2 coating was higher than subsequently obtained with current collecting stripes.

Data was also taken on the performance of this back wall film cell as a function of temperature at temperatures above room temperature. The cell was mounted on a temperature controlled hot plate and illuminated with a tungsten lamp at simulated sunlight intensity. The temperature was measured with a thermocouple and I-V characteristic curves were taken at different temperatures in the dark and under light. Figure 8 shows the variation in open circuit voltage with temperature, while Figure 9 gives the variation in short circuit current with temperature. In Figure 10 we have plotted the power output and the open circuit voltage-short circuit current product as a function of temperature. This particular cell was not an outstandingly high efficiency cell, but it was typical of back wall film cells on conducting glass substrates that were fabricated earlier in the contract. It is seen that the open circuit voltage showed a linear drop with temperature from room temperature to 150°C. The slope of the curve represents a drop in voltage of 1.32 mv per °C rise in temperature. Previous measurements on single crystal cells showed a drop of about 1.64 mv/°C. It is probable that this difference is statistical rather than a significant difference between single crystal and film cells. The short circuit current versus temperature curve shows an apparent discontinuity at about 85°C. The current appears relatively constant at temperatures below this point and shows an exponential drop with absolute temperature above this point. The slope of the drop gives a variation in current with $T^{-1.385}$.

From 20°C to 175°C the power output drops from 7 mw to a little over 2 mw, or to 28.5% of the room temperature value. The open circuit voltage-short circuit current product dropped from 16 to 6 mva over the same range, or to 27% of the room temperature value. However, though the overall drop for the 2 curves is approximately the same, the rate at intermediate temperatures is widely different. This indicates appreciable differences in the rectangularity of the I-V characteristic curve at different temperatures.

Stability

The CdS evaporated film photovoltaic cell has shown short term indications of far greater stability than CdS single crystal cells. Part of this difference may be due to the fact that lower initial efficiencies are obtained from the film cells, and lower efficiency cells might well be less subject to atmospheric effects. However, the film cells have shown some decay when exposed to ordinary room atmosphere.

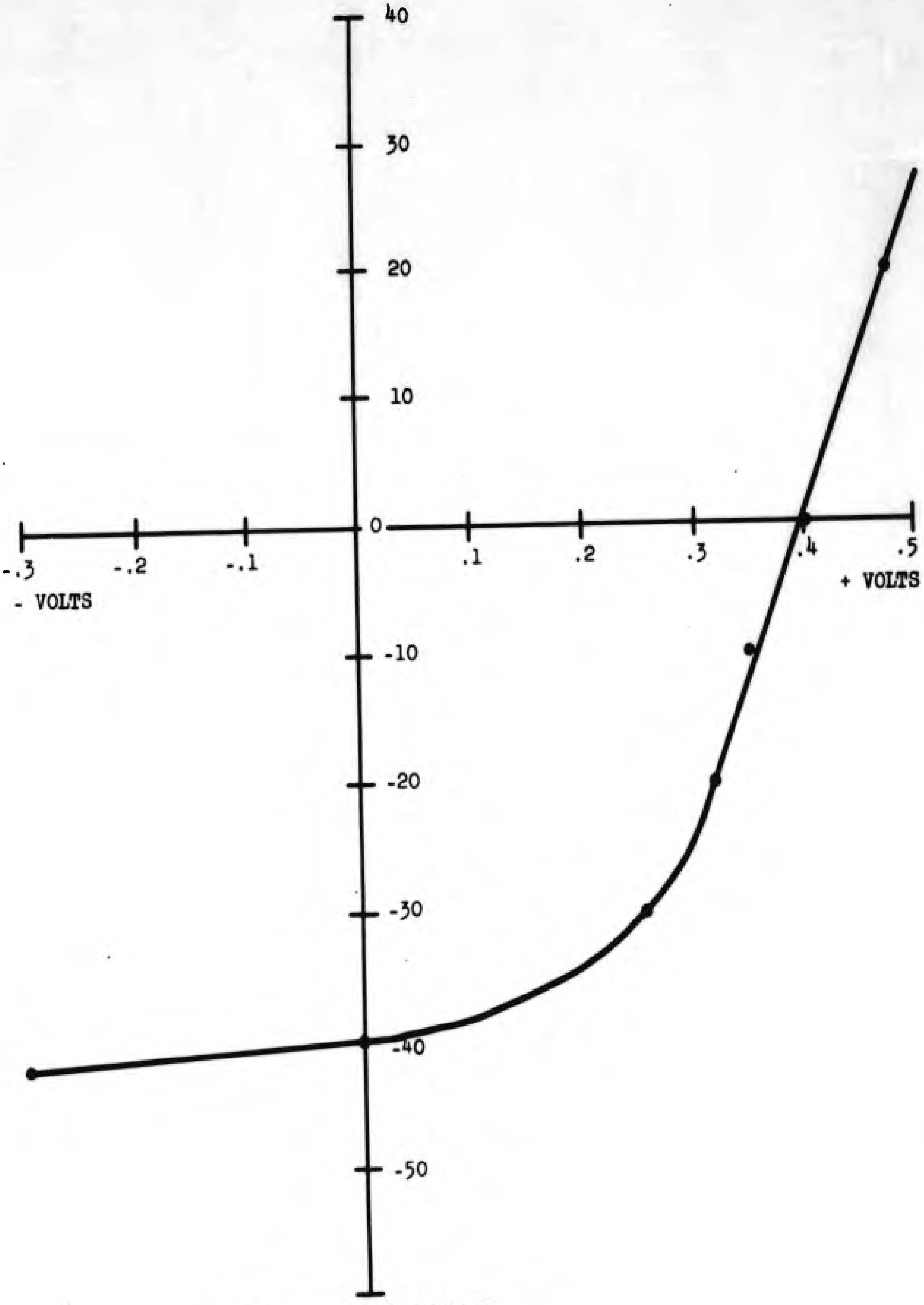

FIGURE 7

I-V Characteristic Curve - Evaporated CdS Film Cell on Glass

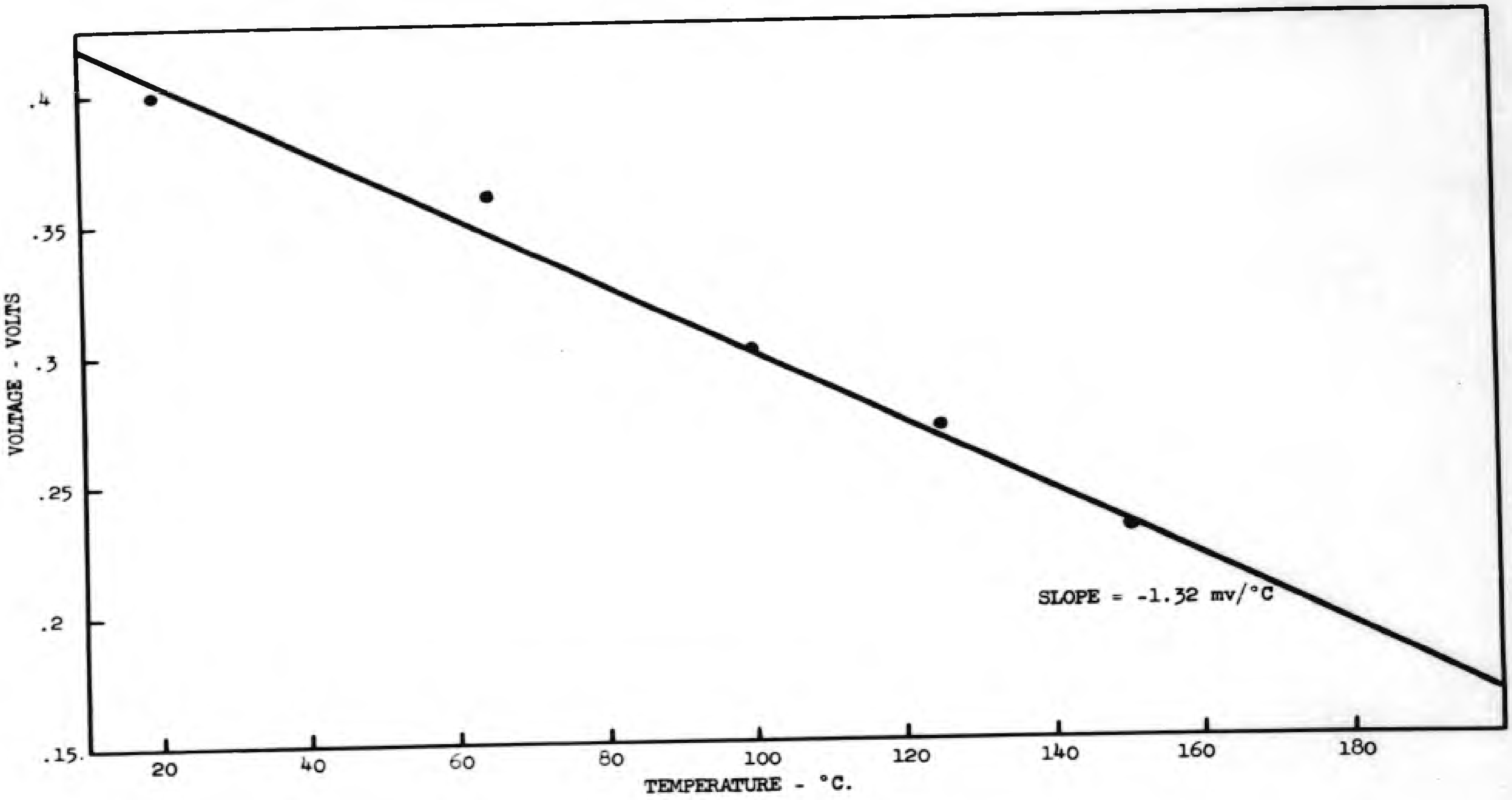

FIGURE 8

Open Circuit Voltage vs Temperature - CdS
Evaporated Film Cell on Glass Substrate

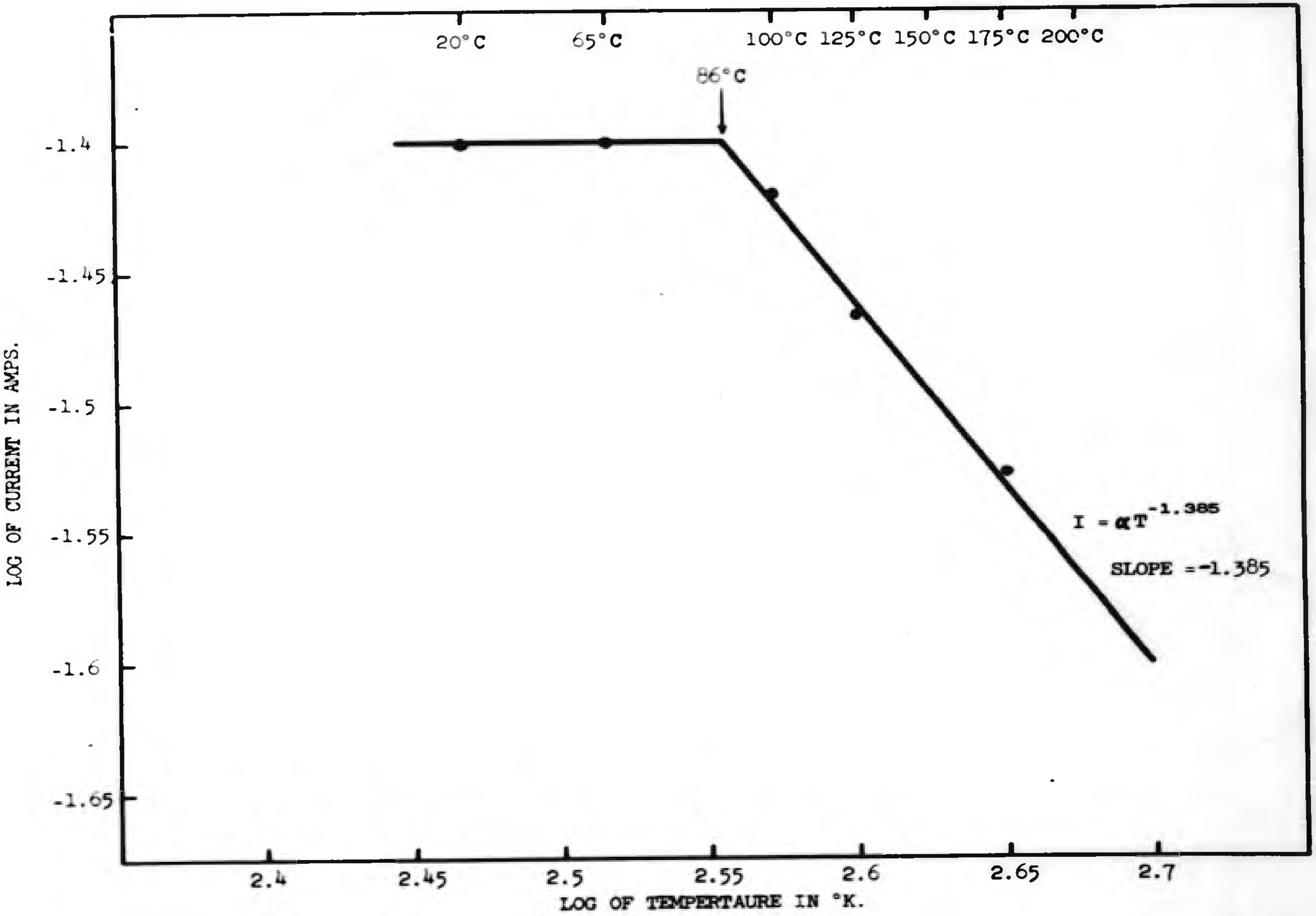

FIGURE 9

Short Circuit Current vs Temperature - CdS
Evaporated Film Cell on Glass Substrate

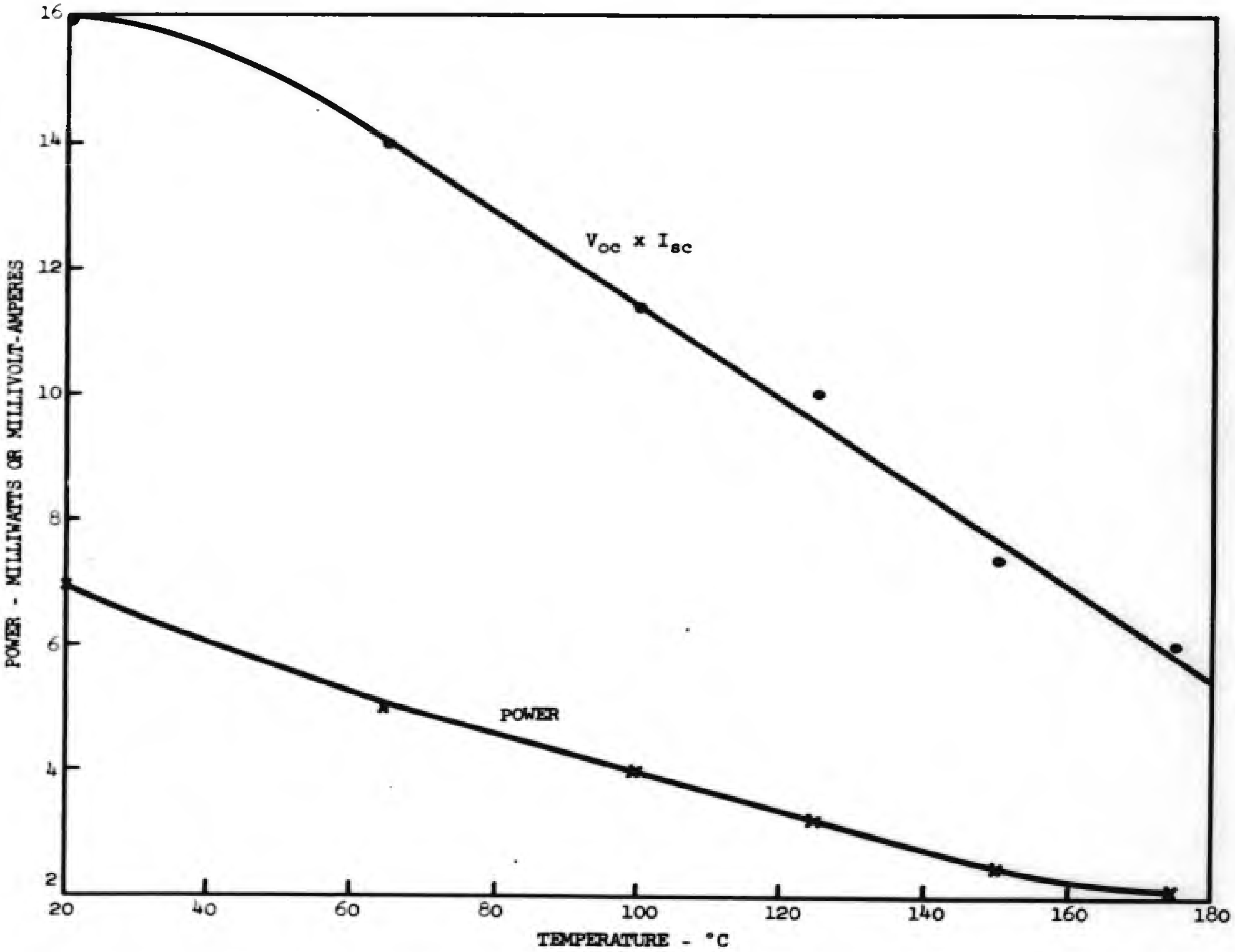

FIGURE 10

Output Power and Voc x Isc vs Temperature - Evaporated Film Cell on Glass

Laminating the cells in various plastic envelopes apparently slows the rate of fall off in output power, and the degree of such slowing seems, from very preliminary data, to be dependent on the relative degree of moisture impermeability of the particular plastic used. Thus Kel-F provides appreciably greater protection than polyethylene, and thick layers of Kel-F provide more protection than thin layers.

Life tests of arrays laminated in various plastic materials have been run at most for three months for the first tests, and for only a few weeks for the later tests. Some laminated cells have been stored in dessicators, and some have been hermetically sealed in vacua of about 10^{-5} Torr. The dessicator storage tests have been on for about a month and the cells and arrays appear to have held their power output or even to have improved slightly. Likewise, those hermetically sealed in vacuum have been on for only 2 weeks but appear to be holding up without measurable loss in output.

It therefore is at least initially indicated that the CdS evaporated film cells are stable except when water vapor is present. This was essentially the experience with single crystal cells after as much as 2 years storage. Further tests for longer periods are of course needed.

PART II - BASIC SUPPORTING RESEARCH

OBJECTIVES

During the course of this investigation, it was realized that in addition to developmental efforts, a fundamental approach would be necessary to improve the CdS photovoltaic cell. The achievement of immediate goals was hampered by several unknown factors which could not be provided through the experience and evaluation from development. Accordingly, basic research was stressed in several areas which were considered to offer possibilities of yielding fruitful results. Foremost among these were ideas for deriving higher cell efficiencies, better reproducibility of materials or procedures and eventually, a comprehensive operational understanding of the cell.

The material aspect of cell production was confined to detailed studies on single crystals and films. Factors which could influence the characteristics of a uniformly prepared cell included the following:

1. Variations in the stoichiometry of CdS,
2. Orientation and surface barrier interface morphology,
3. Dislocation and other defects in the cells.

All of the above could also strongly influence the electrical behavior of CdS before barrier application.

Next, the barrier itself has to be examined from the viewpoint of composition of the surface layer, novel techniques of formation, and interactions with the CdS base material. Of necessity, this involved numerous quantitative measurements on isolated portions of the cell. Equally important were many of the parameters of finished cells normally determined by electrical and optical procedures. Some valid conclusions regarding the active barrier and how it formed were reached and experimentally verified.

Worthy and significant theoretical analysis was provided by consideration of the final cell as operating via a surface barrier photovoltaic effect. New hypotheses contributed to and stimulated the concurrent experimental work. Eventually a model for CdS cell operation was proposed and served to explain characteristic data in a nearly quantitative manner. As yet no maximum output efficiency has been rigorously derived, but further refinements in theory may predict outputs of the order of those observed.

SINGLE CRYSTAL AND FILM STUDIES

Single Crystal Growth and Annealing

It has been consistently found that undoped CdS grown in an inert atmosphere at 1200-1300°C or in a vacuum at 800-900°C has a resistivity in the range of 1-10 ohm-cm. This is believed due to sulfur deficiency in the CdS crystal leading to sulfur vacancies and/or cadmium interstitials, both of which would contribute donors and give n-type conductivity. It has been reported by Kröger, Vink and Van den Boomgaard(9) that high resistivity CdS can be grown in a sulfur-containing atmosphere. In order to examine the properties of CdS crystals in a reproducible state, an attempt was made to postanneal undoped CdS crystals in sulfur atmospheres. Several runs were carried out. In these cases the temperature of the CdS was kept at 900°C and the sulfur at 220°C, in a two-temperature furnace. Several runs yielded material of 10^7 ohm-cm to 10^9 ohm-cm and higher in the dark and 10^5 to 10^6 ohm-cm in the light, with a light-to-dark ratio of 10^2 to 10^3. These results have been compared with untreated samples from the same lots which had resistivities of 2.40 ohm-cm and were not photoconductive.

CdS crystals were also grown in an H_2S atmosphere following the procedure used by Czyzak *et.* *al.*(10) Under these conditions, three reactions take place.

1. $\mathrm{H_2S(g)} \rightarrow \mathrm{H_2(g)} + \frac{1}{2}\mathrm{S_2(g)}$,

2. $\mathrm{H_2(g)} + \mathrm{CdS(s)} \rightarrow \mathrm{Cd(g)} + \mathrm{H_2S(g)}$,

3-a. $\frac{1}{2}y\mathrm{S_2} + \mathrm{CdS}_{(1-y)}\Delta y \rightarrow \mathrm{CdS}$,

3-b. $\frac{1}{2}y\mathrm{S_2} + \mathrm{Cd}_{(1-y)}\ \boxed{\mathrm{Cd}}\ {}_y\mathrm{S}_{(1-y)} \rightarrow \mathrm{CdS}$.

Here Δ and $\boxed{\mathrm{Cd}}$ represent tetrahedral sulfur vacancies and cadmium interstitials respectively. Reaction 1 was studied by Gordon(11) in detail. Utilizing his values for the equilibrium constant at various temperatures, the degree of dissociation can be computed for 1285°C. It was at this temperature that the CdS crystals were grown, and approximately 25% of the H_2S was dissociated. Reactions 2 and 3-a are apparently slow, and the predominant effect then is 3-b. Undoped growth runs in H_2S were made with total pressure of H_2S at one atmosphere. The liberation of sulfur was demonstrated by deposits in the outer regions of the growth tube. Spectrographic analyses were similar to those of undoped crystals. Optical transmission in the infrared indicated a purity equal to that of argon-grown materials. The dark resistivity was in the order of 10^8 to 10^{11} ohm-cm, or about 10 orders of magnitude higher than that of argon-grown crystals. This clearly demonstrated that the high conductivity normally experienced was due to sulfur deficiency. This result indicates that the H_2S-atmosphere-grown crystals either contain a very small amount of electrically active residual donor impurities in the standard CdS material, or show the strong influence of sulfur deficiency or cadmium excess, which would also cause electron conduction. The residual impurities in CdS have been analyzed by mass and optical spectrometry as reported on pages 1 to 6. The reported presence of traces of some donor and acceptor atoms would lead to either increased conduction or compensation. Exact effects could only be ascertained by measuring properties of ultrapurified CdS.

Etching and Orientation Studies on Single Crystals

The sphalerite structure, which includes the II-VI compounds, differs from the diamond structure only in composition. In the elements carbon, silicon, germanium and tin, with the diamond structure, every atom is bonded to four other atoms of its kind. In the sphalerite type structure (e.g. cubic CdS) every atom A is bonded to four of another kind, B, and vice versa. The crystallographic difference is largest when (111) and $(\bar{1}\bar{1}\bar{1})$ planes are compared. The upper layer of (111) is composed of A atoms while the upper layer of $(\bar{1}\bar{1}\bar{1})$ is composed of B atoms. The slowly attacked tetrahedral plane which assumes a negative charge upon pressure normal to it, is defined as (111). A similar picture holds for the related wurtzite (hexagonal CdS) structure with respect to the (0001) and $(000\bar{1})$ planes. Thus the basal plane, which is attacked most slowly by HCl, HBr, HI and many other etchants and which assumes a negative charge for pressure normal to it, is defined as (0001). In this way, the crystal orientation can be determined by etching and subsequent analysis by the light figure technique.(12) The resulting light figure reflections from the etched crystal surface are shown in Figure 11.

In an effort to determine the effect of orientation of CdS photovoltaic cells, one large CdS single crystal was oriented and a slice about 2 x 20 x 20mm was cut parallel to the (0001) plane. The orientation was done by the light figure method. With the wurtzite structure the (0001) plane side (of which the upper surface layer consists of cations) appears flat and specular, while the $(000\bar{1})$ plane side (anions uppermost) appears matte. A piezoelectric test confirmed the direction of orientation. Upon compression, in the "c" direction, a positive charge forms on the $(000\bar{1})$ side (sulfur atoms uppermost) and a negative charge forms on the (0001) side (cadmium atoms uppermost).

This oriented slice of standard .003% $InCl_3$-doped CdS was then cut in half and single crystal photovoltaic cells fabricated from each half. On one piece, the barrier was placed on the (0001) plane surface and on the other it was formed on the $(000\bar{1})$ plane surface. The I-V characteristic curves were taken and plotted in Figure 12. Curve 1 is a plot of the forward voltage-log current curve, in the dark, of a cell with the barrier on the $(000\bar{1})$ surface. This is fitted by the equation:

$$(000\bar{1})\ I_{dark} = 1.8 \times 10^{-10}\ (\exp\ (qV/1.87\ kT)\ -1) \text{ in amps/cm}^2.$$

Curve 2 is the same cell in simulated sunlight, plotting forward voltage against log of current +3.6 ma/cm^2. (The cell produced an open circuit voltage of 0.52 volts and a short circuit current of 3.6 ma/cm^2.) The curve is fitted by the equation:

$$(000\bar{1})\ I_{light} = 3.6 \times 10^{-3} - 3.3 \times 10^{-4} (\exp\ (qV/8.5\ kT)\ -1).$$

Curve 3 represents the dark characteristic of the cell with the barrier on the (0001) face. It is fitted by the equation:

$$(0001)\ I_{dark} = 9.75 \times 10^{-6}\ (\exp\ (qV/3.9\ kT)\ -1).$$

Curve 4 is the same cell in simulated sunlight with the forward voltage plotted against the current, plus 3.6 ma/cm^2. Open circuit voltage was .50 volts for this cell, and short circuit current was 3.6 ma/cm^2. The following equation fits this curve:

$$(0001)\ I_{light} = 3.6 \times 10^{-3} - 4.2 \times 10^{-4}\ (\exp\ (qV/9\ kT)\ -1.$$

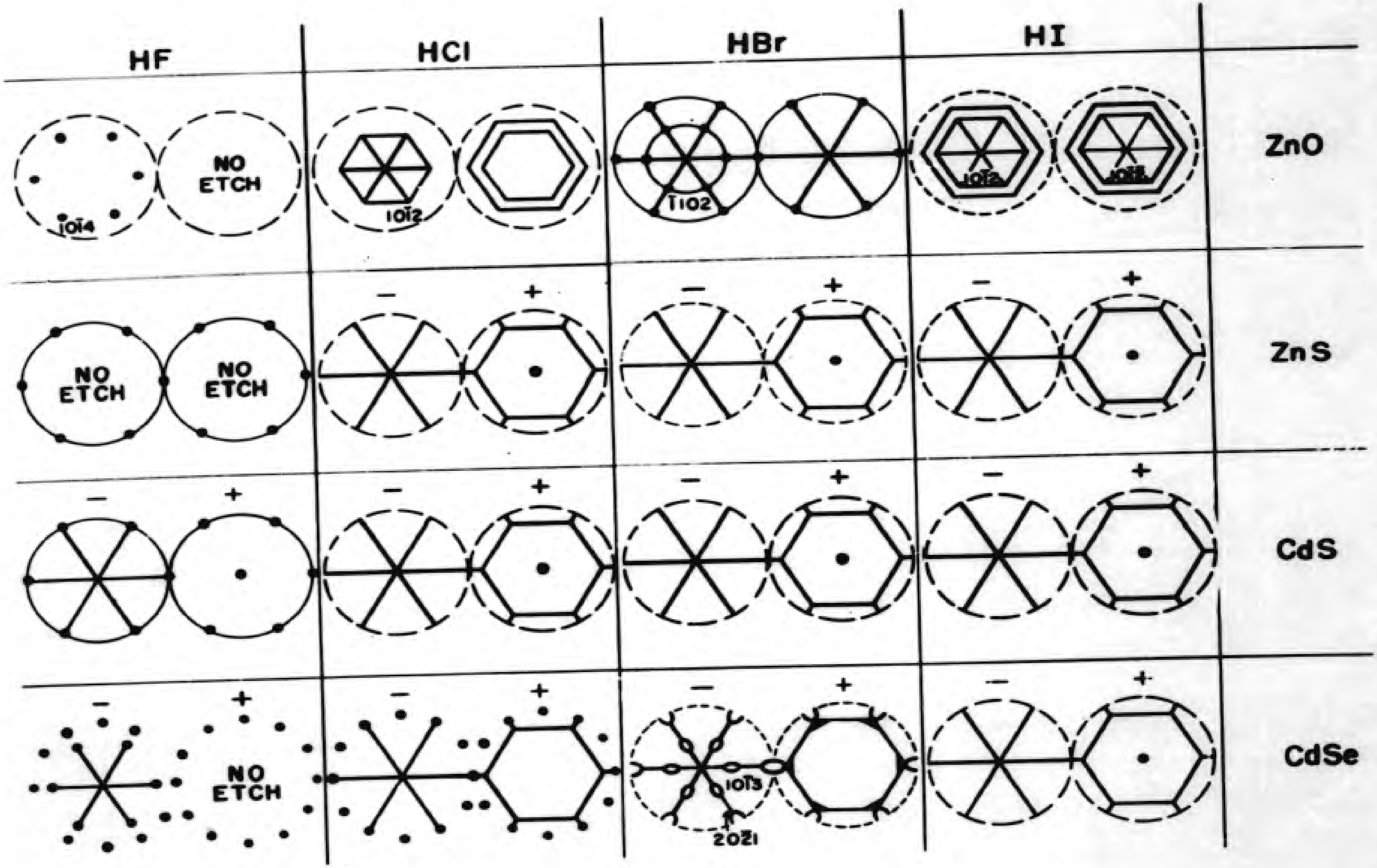

FIGURE 11

Stereographic Projection of the Most Slowly Attacked Planes in Wurtzite Structure Materials

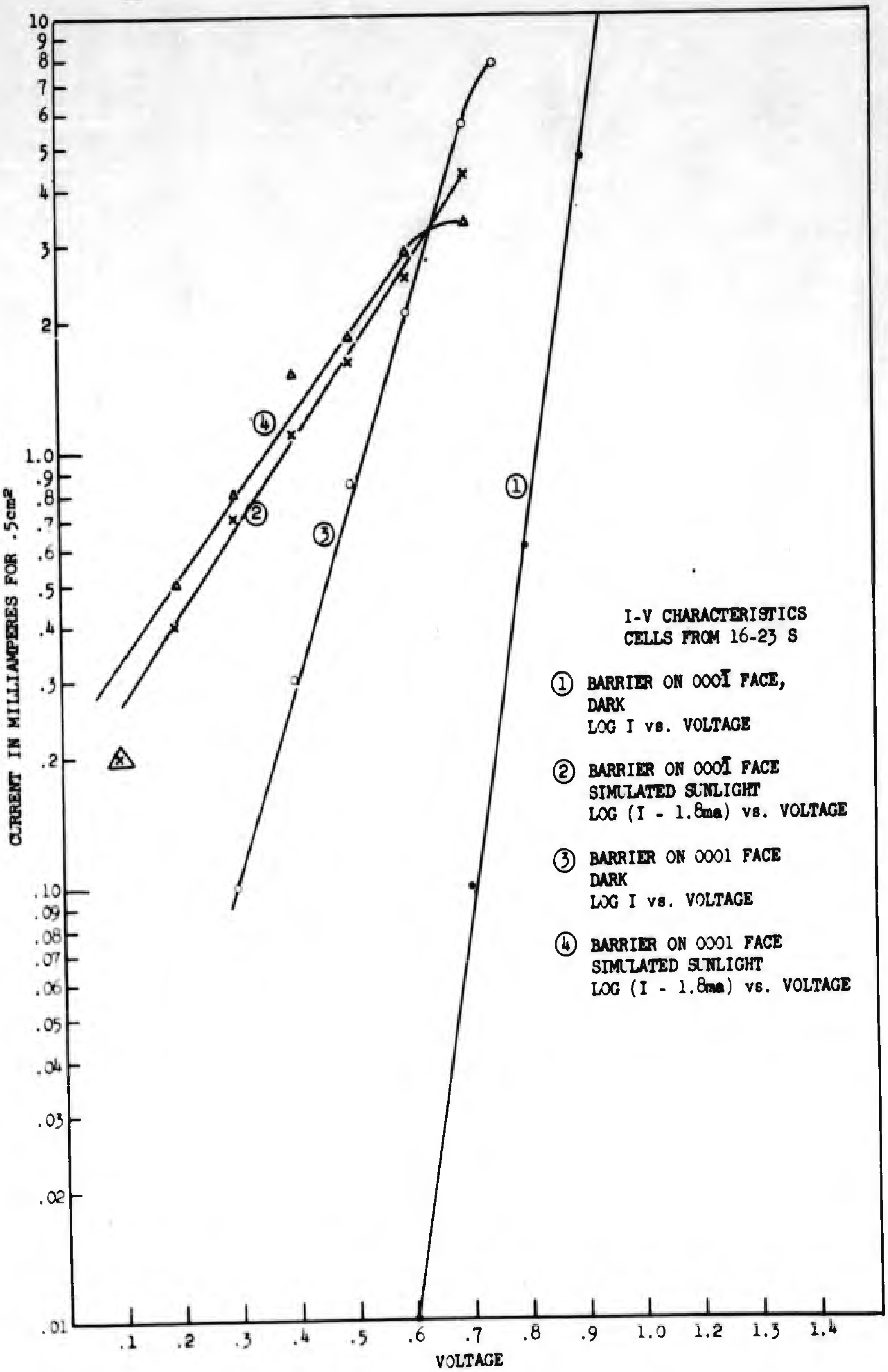

FIGURE 12

Light and Dark I-V Characteristic Curves for CdS Cells with Barriers on 0001 and $000\bar{1}$ Surfaces

The cells were nearly identical in simulated sunlight, there being only minor differences in the saturation current term and the constant in the denominator of the exponent. The short circuit currents were the same and there was a slight difference (4%) in the open circuit voltage. We can tentatively say, therefore, that as far as solar energy conversion is concerned, the orientation of the crystal between the $[0001]$ and $[000\bar{1}]$ directions was of no consequence.

In the dark, however, it was apparently of considerable consequence whether the barrier was placed on the (0001) or $(000\bar{1})$ surface. The saturation current term was different in the two cases by a factor of 2×10^5 and the constant in the denominator of the exponent by a factor of about 2. This would seem to indicate that other differences might be found in other characteristics, such as spectral response and response at low light levels.

Grain Growth of CdS Films

An attempt was made to increase the grain size of CdS films after the method of Gilles and van Cakenberghe.(13) Films of CdS on pyrex substrates were coated with approximately 20 Å of silver by vacuum evaporation and heated in argon atmospheres at 500-600°C for several hours. These films showed large grains of size up to 1 to 2 cm across, but the growth was very dendritic; similar in appearance to frost forming on a cold window pane.

Better results were obtained when the silver was placed on the slide and the CdS film evaporated onto the silver. These slides had smaller grains, up to somewhat less than a centimeter across, but the grains were not so visually apparent except under polarized light. There was no evidence of the dendritic or "frosting" type of structure observed in the earlier test.

An initial attempt to make cells from slides treated as above was not successful. Difficulty was encountered with the copper from the barrier plating operation penetrating mainly along the grain boundaries. After heat treatment, these cells had no output and behaved as though they were shorted.

Red fluorescence was observed from those slides when excited with long wave length UV, indicating that some silver had diffused into the CdS. Since the luminescence was of low intensity, it was believed that the amount was not great and probably not sufficient to compensate the CdS to any marked degree, as far as n-type conductivity is concerned.

Dislocation Studies and Etching Behavior

The effect of the various types of dislocations and point defects on the electrical properties has been established in many crystal materials. The control of both the point defect concentration and the dislocation density in CdS was therefore necessary. It appears now that an electrically comparable starting material can be reproducibly made by the treatment with sulfur from H_2S at elevated temperatures. This treatment essentially controls the intrinsic point defects; namely, mostly Cd and S vacancies and interstitials, while the dislocation density in the various samples appears comparable. Since screw dislocations are expected to be electrically inactive, the investigation was mainly aimed at the influence of the edge dislocations. The most important edge dislocations will be the ones that can be produced by the utilization of (0001) as a glide plane. These dislocations are appropriately called 60° dislocations. There would exist two types of them: 1) the 60° dislocations containing triply bonded cadmium atoms which are expected to act as acceptors, and 2) the corresponding S dislocations which are expected to act as donors. It is also expected that annealing of the crystal will reduce the number of these dislocations; this treatment will not remove them completely, however, because of interlocking and polygonization. Electrically, the Cd and S dislocation lines, parallel to the three a-axes, will behave as cylinders of negative and positive space charges respectively, and will favor breakdown effects. For the purpose of this investigation, CdS (0001) single crystal plates have been bent parallel to the a-axis in both directions at 1100°C, so that the crystal surface appears concave or convex (of about 5 cm diameter) with respect to (0001). Concavity and convexity of (0001) produces Cd and S-edge dislocation lines, respectively. The change in charge carrier concentration in these crystals was too small to be detected, however, since it appeared that the initial concentration of dislocations was too high. For structural and orientational reasons, the influence of these dislocations on the photovoltaic properties of the film cell was very likely small, since the orientation of the crystallites, as has been found, on the average was parallel to the film. Wide deviations from this orientation, however, could result in the failure of the film in some locations.

"Neutral" dislocations are another type of edge dislocation. These are parallel to the c-axis and differ from the 60° dislocations where $[11\bar{2}0]$ is an acceptor or donor line in that this [0001] dislocation line represents a compensated Cd and S acceptor-donor line. Here the triply bonded Cd and S atoms alternate. It thus will not influence the conduction type, but it certainly will influence the life-time properties. These dislocations can most easily be revealed upon etching of (0001) with dilute HCl. (Figure 13).

Prior to the investigation of the various dislocations in CdS it appeared necessary to study the etching behavior of this compound. When the concentration of impurities was high, the etching characteristics indicated a dendritic structure, which at the same time was indicative of a high dislocation content (Figure 14). Dendritic growth appears when the supersaturation of the solvent (CdS) in the matrix (CdS vapor phase) is high; it is characterized by branching and tree-like formations. This type of growth is controlled by the dissipation of the heat of deposition or, mostly, as in this case, the diffusion of the required material. It is often preceded by needle-type (and sometimes plate-like) growth. Protrusions, which extend from the surface, in a given crystallographic direction, appear on the lateral surfaces of the primary needle almost equally spaced. These grow into branches which then develop secondary branches in the same way. In this way, the spaces between the dendrite branches are filled in at the end of the solidification process. Dislocations then occur when, during the "filling in" process, there is an imperfect meeting of the neighboring branches. It is characteristic of this type of growth that, with each material, there is associated a dendritic axis of low index. So pronounced is this feature that dendrite axes are used to orient crystals. For CdS crystals, the a-axis appears to be the dendrite axis. For the growth of good crystals, dendritic growth is to be avoided. Dislocations can be brought out quite

Magnification Approx. 150X

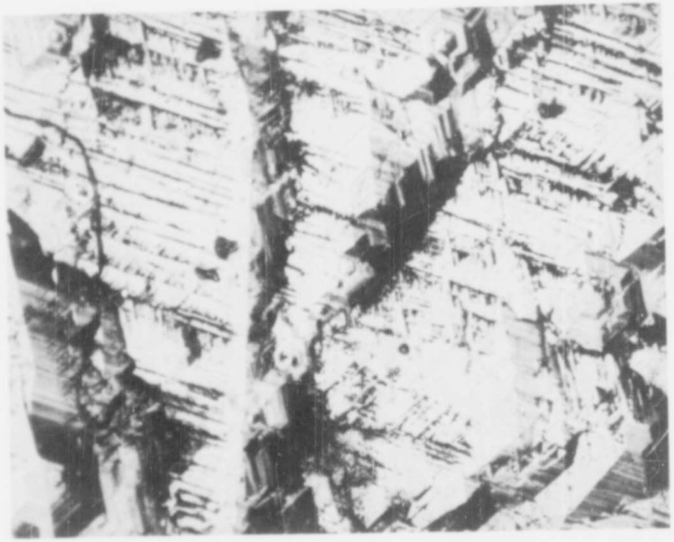

(00.1) Plane Etched Five Hours in Dilute (1:1) HCl

FIGURE 13

Etched CdS Crystal Showing Dislocations

Magnification Approx. 150X

Etched 3 Days in Dilute (1:2) HCl at Room Temperature

FIGURE 14

Etched CdS Crystal Showing Dendritic Structure well by chemical etching (see also D.C. Reynolds and L.C. Greene(14) and J. Woods(15)) provided the dislocation concentration does not exceed a certain value which varies from substance to substance.

In Figure 13, the dislocation lines intercepting (0001) are aligned in the direction of the a-axis. They would represent "neutral" edge dislocations. The two types of edge dislocations are shown in Figures 15 and 16.

The following principles may be used as a guide in the selection of a dislocation etch. Since dislocation pits appear where dislocation lines and slowly attacked planes intercept, the selection of proper etchants and oriented surfaces will lead to good results. For this purpose a slow etch must be applied to the resistant F-planes (F denotes "flat"). For example, using aqueous HCl as an etch to CdS, the solution must be applied dilute to either (0001) or to $(10\bar{1}\bar{1})$.

There is much misunderstanding on etch pit habit as revealed in the literature.* The misunderstanding mostly stems from the lack of distinction between the etching of concave and convex curfaces. The etching of concave surfaces results in truly polyhedral forms. The etching of convex surfaces, on the other hand, results in the geometrical forms ("solution forms") which are bounded by curved ridges which in turn represent slowly attacked crystallographic planes (S, or stepped planes.) The latter are parallel to only one bond chain in a similar sense as defined above for F-planes. These ridges then intersect in F-planes which are parallel to more than one bond chain. Although experimental complications make the understanding more difficult, the picture is fairly well described by the preceding outline. As an appropriate example, the (convex) solution form of CdS etched in concentrated HNO_3 for 1 minute is shown in Figure 17. In Figure 18, this form is schematically shown together with the corresponding (concave) etch habit form. In Figure 19, the corresponding form (and/or light figure) is given in stereographic projection.

Since the dislocation pits are supposed to be characterized by a pyramidal etch pit habit, it follows that pyramidal pits can also be obtained when no dislocations are present. When, for instance, a protective and truly adhering layer on $(000\bar{1})$ is penetrated by an HCl etchant, pyramidal etch pits will invariably be formed. In these experiments, other etchants, including H_3PO_4, HBr and HI have been tested. The most favorable procedures for a dislocation etch appeared to be thermal etching, etching in aqueous solutions of H_2CrO_4 and H_2SO_4, HF, HCl and $(CH_3)_2N(CH_2)_3NH(CH_2)_2CN$, HCl + $(C_2H_5)_3NHCl$, HCl + + $[(CH_3)_2N]_4B_2$.

There are two theoretical approaches to interpreting etch forms which can stand up to a critical scrutiny, namely the kinetic and the thermodynamic approaches. Although in this case there is apparently no direct correlation between the two approaches, their results cannot contradict each other. Since the kinetic analysis is quite elaborate, it will not be given here. The thermodynamic

---

[*] For a further, detailed discussion on etch pit habit and on etching of convex and concave crystal surfaces, consult reference (25).

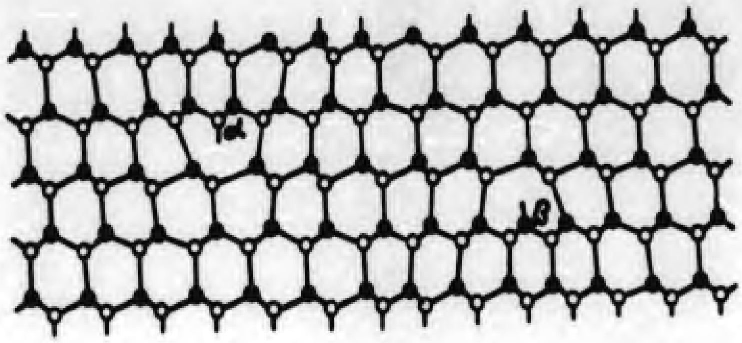

FIGURE 15

60° Dislocations, α and β Types: Projection on(11.0)
(Open Circles Cd Atoms - Full Circles Sulfur Atoms)

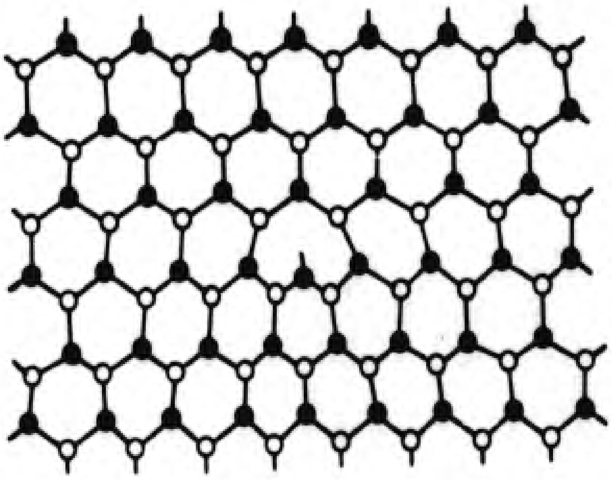

FIGURE 16

"Neutral" Dislocations: Projection on (00.1)
(Open Circles - Cd Atoms, Full Circles - S Atoms)

The atoms alternate in the direction normal to the projection.

a - Top View (Cd-Side) Mag. 4X

Uppermost Top Represents (00.1)
Six Lines Which Are Parallel to
the A-axis Represent (h) .1 Planes

b - Side View Mag. 4X

Intersection of Ridges
are (10.1) Planes

c - Bottom View (S-Side) Mag. 4X

FIGURE 17

Solution Form Photomicrograph of CdS
(Etched One Minute in Conc. HNO_3)

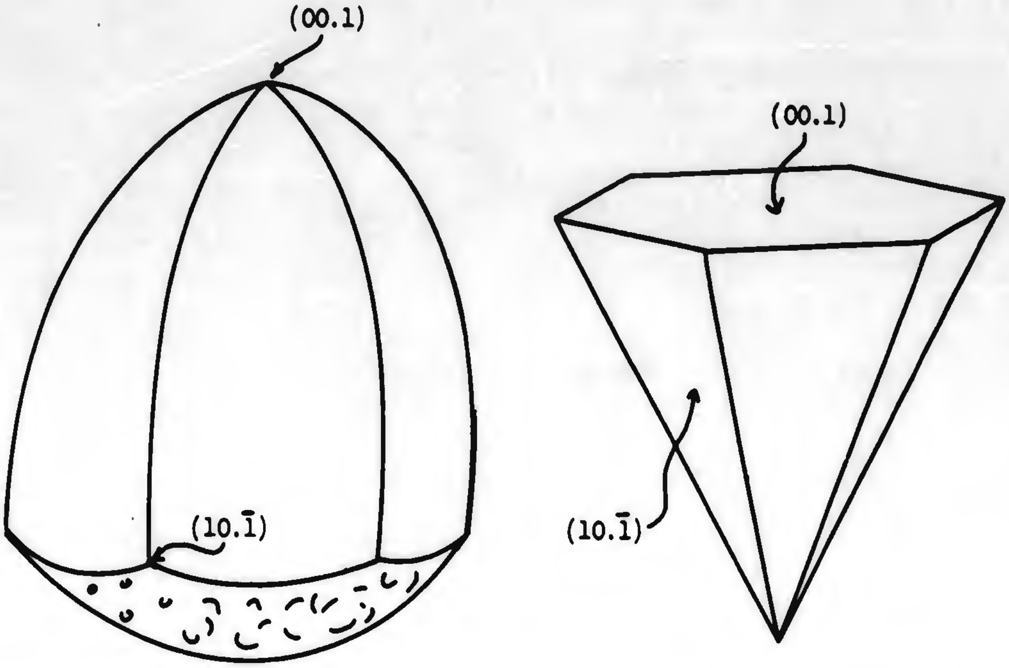

a - Convex or Positive

b - Concave or Negative

FIGURE 18

Schematic Drawing of Rounded Solution Form
and Corresponding Polyhedral Etch Pit Form in CdS

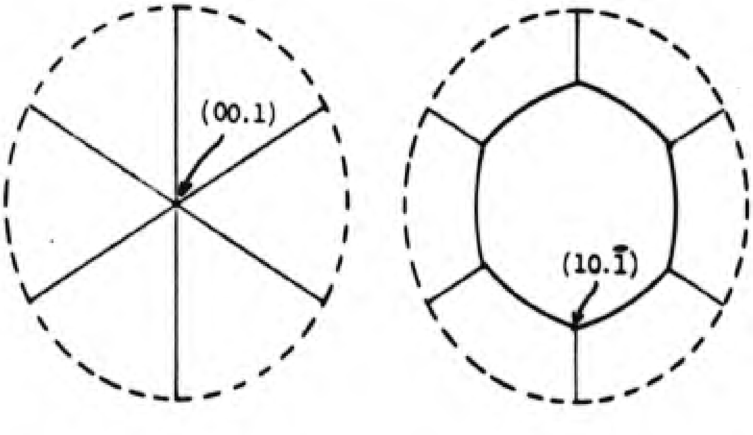

FIGURE 19

Stereographic Projections Representing Both Rounded
and Polyhedral Etch Pit Forms in CdS

(Crystal Edges of Adjoining Crystal Faces of polyhedral forms are shown in the projections as lines connecting those planes. The projections also represent the corresponding light figure patterns of CdS etched in HCl, HBr, HI, HNO_3, H_2SO_4 and H_3PO_4 as described in the text.)

approach is based on Gibbs' and Wulff's laws governing the equilibrium forms of crystals. Again, going into the various aspects of the related theory would require extensive details. Therefore, only the final results in the form of the derived theoretical habits in stereographic and clinographic projection in Figure 20 are given. The various habits are found for wurtzite structure materials when the respective cations contribute in different amounts to the surface energy. From comparisons with actual habits observed, it is concluded that for ZnS (wurtzite) the ratio γ of anion to cation contribution is less than one-third, and for CdS (greenockite) it is less than one but greater than one-third. In the etch forms of hexagonal ZnS, CdS and CdSe obtained from HCl, HBr and HI etching, and also in the etch forms of CdS obtained by etching in HNO_3, H_2SO_4 and H_3PO_4, the situation is reversed. By the interaction of the etchant, the "cation atoms" (Zn, Cd) become stabilized so that now they contribute less than one-third to the surface free energy than do the "anion atoms" (S, Se). If confirmed, an important result of this investigation is that on the CdS surface S_8, S_6 rings or S chains are strongly adsorbed onto CdS arrays parallel to the z-axis. This effect would tend to lower the hemihedral properties of this compound.

EXPERIMENTAL WORK ON THE PHOTOVOLTAIC BARRIER

Analysis for Copper at Various Stages of Cell Formation

Several slabs of CdS were plated from a standard acidic (copper) plating bath in the usual way(16), except that small quantities of the bath were used. The plating solution was analyzed for Cd. Of several slabs that were subsequently made into cells, some had the loose excess of material normally present after heating, scraped off. All the cells were analyzed. The results were reported by the analyst as indicated in Table VII.

It can be said with confidence that about 10^{17} Cu atoms are incorporated integrally with the CdS, either by diffusion into the material or as a strongly bound film. Also, it must be realized that if such a film of metallic copper existed it could be only of the order of .1 micron thick.

The next question arose: Is there, or is there not, a real diffusion of copper into the CdS following a heat treatment? To determine this, the surface of the CdS was successively ground away, a fraction of a micron at a time. The thickness lost was determined by weighing. After each grinding, the CdS was examined for Cu by x-ray fluorescence. The analyst reported that there were indeed traces of Cu in the crystal at depths of as much as 5 microns.

As a criticism of the analysis, it must be said that the results are expected to be in error because both measurements, the thickness measurement and the differential copper measurement, involve small differences of large numbers. In addition, all measurements that were taken involved methods at the limit of their sensitivities. Further, as it became evident that the process of CdS removal, namely grinding, involved roughening the surface to an extent greater than the reported depth of diffusion, the reported diffusion depths were abandoned.

a - for $\gamma \geqq 3$ (for $\gamma \geqq 1/3$; ℓ is replaced by $-\ell$)

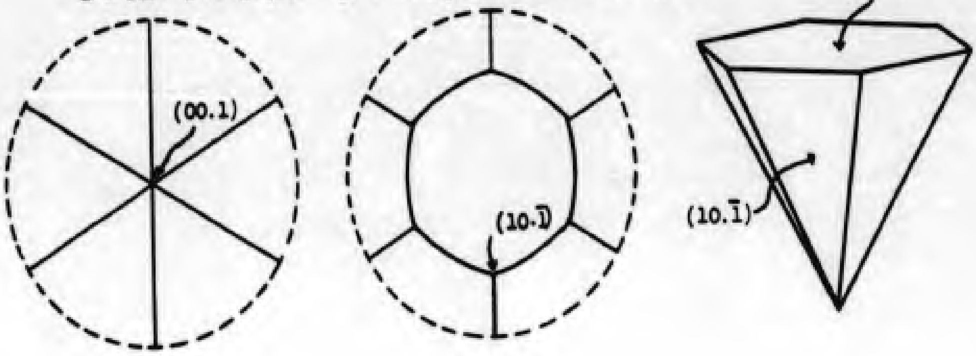

b - for $3 > \gamma > 1$ (for $1/3 < \gamma < 1$; ℓ is replaced by $-\ell$).

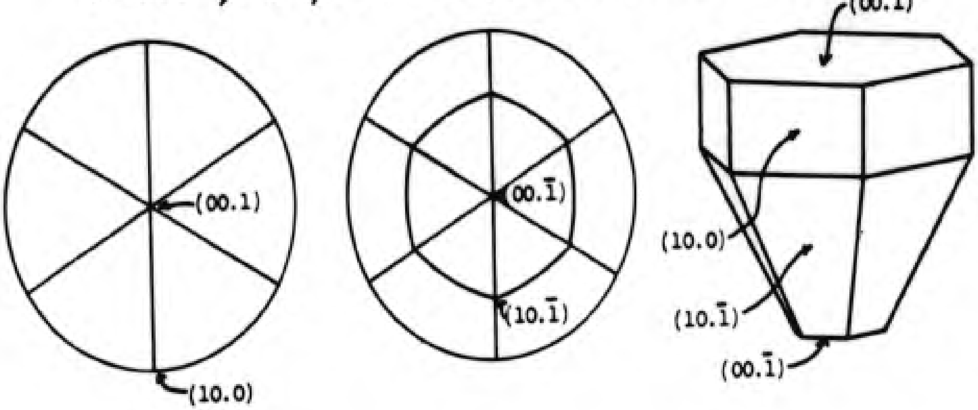

c - for $\gamma = 1$.

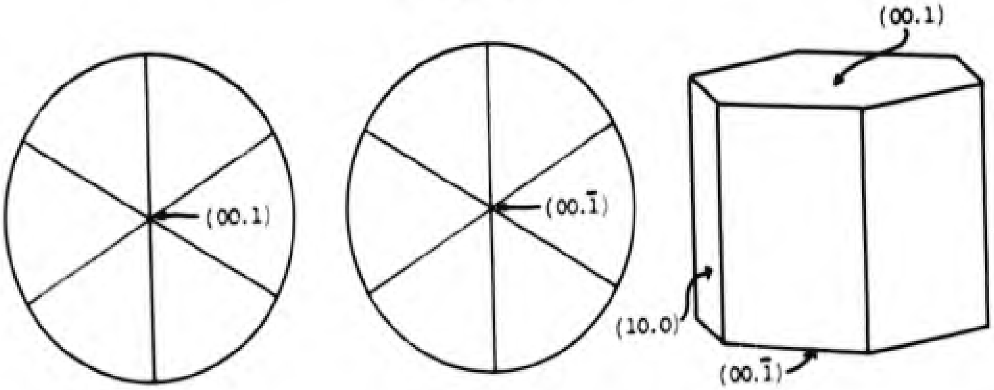

FIGURE 20

Stereographic Projection and Clinographic Projection of Crystal Forms of Wurtzite Structure for the Various Ratios of Anionic to Cationic Contribution to the Surface (or Interface) Free Energy

TABLE VII

THE ANALYSIS OF THE CdS AND PLATING SOLUTION, FOLLOWING PLATING FROM A Cu BATH AND HEATING (Referred to 1 cm^2)

Cu removed from solution = 3.13×10^{18} atoms.

Cd etched from crystal during plating = 1.89×10^{17} atoms.

Cu present in loose surplus layer = 1.09×10^{18} atoms.

Cu remaining on crystal after removal of surplus = 2.46×10^{17} atoms.

NOTE: The fourth item is to be given more credence than the difference between items one and three, since the analysis is at the limit of sensitivity, and it is believed that a three figure accuracy was achieved.

Much greater sensitivy was achieved by optical microscopic interferometry. A series of CdS crystals was polished to a specular finish, and each was then masked on half of one major surface. The unmasked portion was converted to a photovoltaic cell in the usual manner. Next, the entire crystal was etched in NH_4Cl solution, which dissolves the oxides of copper. On the treated side of the crystal, a reddish-metallic film remained. The Brewster angles of both halves of the CdS crystal were observed. The Brewster angle of the untreated CdS was compatible with a dielectric material, whereas that of the side having the film was so great as to be immeasurable by the techniques available at that time. It was, therefore, assigned to be metallic in character. The thickness of the step between the untreated portion of the CdS and that having the metallic film was measured interferometrically. It was found to be 0.2 microns. In view of the above data, it was reasonable to assume that, after plating from the Cu plating bath and heating to 275°C, no copper diffuses into the CdS to an extent that would affect bulk electronic properties, since there appears to be sufficient copper left on the surface to account for all that was deposited. In fact, the film on the surface was porous in all probability.

Deposition of Copper by Various Methods

Attempts were made to form barriers on CdS single crystal slabs by electroless deposition. Successful electroless deposition of copper on CdS was done when the surface of the CdS was pretreated by a dip into a solution, such as 0.1 g/l $PdCl_2$. However, though a number of samples were prepared using a variety of solutions and reducing agents to give the electroless deposition of copper on CdS, and they all showed some degree of rectification, none showed a photovoltaic effect.

Saubestre(17) suggested a method whereby non-metallic samples could be sensitized by dipping them in a highly alkaline solution prior to immersion in the electroless copper bath. This would eliminate the metallic sensitizer. This method was also tried and copper deposition was obtained. Again, however, no photovoltaic effect was observed. Thus, a simple deposition of copper by itself in a more or less continuous film on CdS does not produce a photocell.

A series of experiments was then carried out on the assumption that Cu_2S was formed on the surface of CdS and thus produced the photovoltaic effect. The initial idea was to remove Cd atoms from the crystal surface and to substitute Cu atoms in their vacancies. The crystal was made the anode using a 12 volt I.D.C. power supply and was dipped into a NH_4OH-CuI solution. A platinum wire was used as the cathode. The crystal was etched for a few minutes and then the bias was reversed and attempts were made to plate copper onto the crystal. Copper layers were not observed, although it was noted that the crystal surface darkened. A comparison of the resistance on the darkened portion of the crystal and on an untreated portion of the crystal with a multimeter indicated much higher conduction on the darker portion than on the untreated portion. After contacts were made to the crystal with silver paint, an electrical check showed that there was rectification and a small photovoltage could be developed when light was shined on the sample.

It was discovered during this series of experiments that the darkening occurred when the crystal was dipped into the solution (CuI:NH_4OH) and that no electrical circuit was required. Electrical checks showed a small photovoltaic effect as well as rectification. Even after leaving a sample in NH_4OH for two hours, the photovoltage could still be observed. A seeming contradiction with other experimental facts arises. Good photovoltaic cells are completely or nearly completely ruined when they are dipped into NH_4OH (see following section). This is attributed to the solubility of Cu_2S in NH_4OH. This seeming contradiction can probably be explained on the basis of magnitudes of the effect in the two experimental procedures. The magnitude of the photovoltaic effect produced by the NH_4Cl-CuI treatment was comparatively small to that of a good cell of comparable area produced by the standard electrodeposition technique.

The same effects have been observed in water solutions of cuprous chloride. The photovoltaic response in this case was slightly greater than that produced using the NH_4OH-CuI solution, but it was still far below that obtained by the electrodeposition process. All purely chemical methods of increasing this effect have not been successful. Solutions with increasing HNO_3 concentrations have been tried with the idea that Cu_2S or CuS might be the cause of the barrier. The effect was not increased. HNO_3 leaves amorphous sulfur on a crystal surface which melts at a rather low temperature. This layer can be spread out evenly over the surface by the proper heat treatment. Attempts to produce a barrier on top of these layers by dipping them into a H_2O-CuCl solution have not been successful. If, however, the crystal is made the cathode and deposition from a H_2O-CuCl-HNO_3 solution is applied, an increased photovoltage is noted. The photovoltage output was nearly equal to a standard comparison sample of the same surface area made by the standard fabrication technique. If the HNO_3 is removed from the solution, a decrease in photovoltaic output is noted. This output was nearly similar to that of samples which were dipped into an H_2O-CuCl solution.

Attempts to produce barriers by dipping in NH_4OH solutions of $CuSO_4$ and $Cu(NO_3)_2$ were negative. No barrier was observed. It appeared, therefore, in confirmation of previous data, that the cuprous ion was necessary rather than the cupric.

Other Investigations on the Nature of the Barrier

Statement of the Problem.

If the photovoltaic cell is considered from the point of view that it is a composite of CdS and an active element, the efficiency might be improved, for example, by increasing the amount of active element if it were not already maximized. It was, therefore, of primary concern to identify accurately this active element. In cell fabrication, one process was that of electroplating copper. This was not sufficient to prove that metallic copper was the desired agent. An attempt, therefore, to improve cell efficiency by increasing the percentage of elemental copper may not lead to the desired results directly, and may even decrease the efficiency if elemental copper was not the desired substance.

There was some experimental data indicating that the cell operation was based on a surface, as opposed to a bulk process; i.e. the active element probably did not diffuse as a dopant into the host CdS crystal(18). The problems to be dealt with, in various degrees of sophistication, were the following:

1. The identification of the active element,
2. The mechanism of its formation,
3. The nature of the physical-chemical bond of the material to the CdS surface,

4. The association of the electrical and photovoltaic properties with this bonding.

Supporting Experimental Data.

Formation of Sulfur on CdS Surfaces.

Several crystals were placed in a solution of 4 parts H_2O to 1 part HNO_3 and allowed to remain in this solution for several hours. When they were removed from the acid bath, the surfaces were splotched with a yellow substance later shown to be sulfur. Several other crystals were simultaneously placed in the barrier plating solution and allowed to remain for a similar length of time. These crystals also showed sulfur on their surfaces when removed from the solution. There were apparent differences in the smount of sulfur left by the barrier plating solution and by the acid solution. The barrier plating solution appeared to etch slightly faster than the acid solution. These differences were small and no great attention was paid to them.

Metal-Sulfur Rectifying Barriers on CdS.

There was some reason to believe that a metal-sulfur compound on the surface of the CdS could form a solar cell, whereas a metal CdS junction would not necessarily form a solar cell. To check this, several crystals were prepared with rhodium contacts. Half of these crystals were then subjected to an etch in an HNO_3 acid solution with an applied current. Nickel was deposited by electroless deposition onto half of these cells, and copper was evaporated onto the remaining half. The same metal deposition was used on the crystals which had not been etched by HNO_3. All were then checked for photovoltaic action and none was found. However, on the cells that were etched and thus had a layer of sulfur on their surfaces, there was invariably a rectifying barrier. Of the remaining cells, some had poor rectifying barriers and most had no barrier.

X-ray Analysis of Plated Deposits.

X-ray analysis of the plated black mossy deposit was carried out in two steps. First, four crystals were plated until a good, uniform-appearing black mossy layer appeared on the surface. The deposit was then scraped from the surface and placed in an X-ray powder camera for a three-hour exposure. The sample was then removed and stored for one week at 105°C. It was then replaced in the X-ray camera and another analysis was made.

Results of the First Exposure.

Metallic copper, cuprous oxide and basic cuprous nitrate were all present and identified positively. The major component was definitely cuprous oxide. This could be misleading, though, since some of the metallic copper may have been oxidized during the three-hour exposure and thus have increased the percentage of Cu_2O.

Results of the Second Exposure.

Cuprous oxide was again detected, and the amount was judged to be the same. However, the lines were much sharper, leading one to believe that the crystal size of the Cu_2O had increased. Basic cuprous nitrate was also detected, but in a much increased quantity over the first exposure. Metallic copper was not detected in this exposure.

X-ray Analysis of the Finished Cell.

X-ray analysis of the surface of the finished cell was also done in two parts. First, after the black mossy deposit turned to straw-yellow color, it was scraped off and analyzed. The remaining surface was analyzed separately. The straw-yellow surface was found to contain positively Cu_2O. The film showed another line which was unidentifiable, but was definitely not metallic copper, CuS or CdS. The remaining surface of the crystal was shown to contain positively Cu_2S. The presence of metallic copper and any oxide of copper were especially looked for, but were not found.

Chemical Removal of Surface Compounds.

In view of the various elements that could be found on the finished cell, it was considered necessary to determine which compound was essential for the operation of the solar cell; i.e., the active agent. It was felt that this task was best accomplished by successive dissolution of compounds suspected to be on the surface. Various standard solvents were used with slight degrees of success. Acetone, isopropyl alcohol, methyl alcohol, toluene and benzene were all used and none affected the performance of the cell beyond anything that could be attributed to mechanical damage. Solutions of NH_4Cl, NH_4OH and KCN provided the most information.

NH_4Cl:

A standard solution of NH_4Cl was prepared and a crystal known to be a photovoltaic cell was immersed in this solution for two minutes at room temperature. It is known that NH_4Cl will dissolve the oxides of copper and the basic nitrate of copper. It will also attack the CdS slightly. After the two minutes immersion in NH_4Cl, the cell was checked for photovoltaic output and found to be substantially the same as before. Thus it was concluded that neither the oxides of copper nor the basic nitrate of copper is essential to cell operation.

NH_4OH:

A standard solution of NH_4OH was prepared and the same crystal as had been used in the NH_4Cl solution was immersed in this solution for two minutes at room temperature. NH_4OH will dissolve the sulfides of copper and the basic nitrate of copper. It will, after a time, attack the CdS. After two minutes in the NH_4OH solution, the cell was again checked for photovoltaic action and was found to have a negligible photovoltage. The basic nitrate of copper had been eliminated as the active agent by the NH_4Cl solution, and thus it was concluded that either a sulfide of copper was responsible for the photovoltaic action or the combined effects of two minutes in NH_4Cl and two minutes in NH_4OH resulted in critical damage to the CdS itself.

KCN:

It had been found previously that a short immersion in KCN will destroy the solar cell. KCN will dissolve both metallic copper and the sulfides of copper, but an anaerobic KCN solution will dissolve only the sulfides. Therefore, an anaerobic solution of KCN was prepared and a cell was immersed in it for a period less than one minute. When the crystal was removed from the anaerobic KCN solution it was kept in a oxygen-free atmosphere and rinsed thoroughly in boiled water. It was then dried and checked for photovoltaic output. There was none. This test was performed on three different known cells with consistent results. It was thus concluded that a sulfide of copper is necessary for solar cell operation on CdS.

Identity of the Active Element of the Barrier.

From the results above, the possible active elements can be narrowed to a sulfide of copper. Henceforth it will be written as Cu_nS_m, where

$$2 \geq n/m \geq 1.$$

Both of the following reactions will occur at room temperature:

$$Cu + S \longrightarrow CuS + \text{energy}$$

and

$$2Cu + S \longrightarrow Cu_2S + \text{energy}.$$

However, the second reaction has the largest change in free energy and will thus be favored thermodynamically. Therefore, it is expected that mainly Cu_2S is present. Furthermore, at the temperature involved in the heat treatment to form the barrier of the CdS cell, namely 275°C, any remaining CuS will decompose according to

$$4CuS + \text{energy} \longrightarrow 2\ Cu_2S + S_2\ \text{(vapor)}.$$

The tentative conclusion reached was that the compound in intimate contact with CdS and essential to the operation of the CdS solar cell was most likely Cu_2S.

Summary of Surface Reactions.

As a summary of the chemical reactions taking place on the surface of the CdS crystal during the fabrication of a solar cell, the following outline is presented:

1. A chemical etch of the CdS by the HNO_3 solution aided possibly by Joule heating, occurs simultaneously with the electroplating of copper on the surface.

2. The first few layers of copper react with the sulfur formed by the etch of the surface to form sulfides of copper.

3. Subsequent deposition of copper results in the formation of a conglomeration of metallic copper, oxides of copper and possible additional sulfides of copper.

4. The heat treatment of the device seems to form additional Cu_nS_m with $n/m \sim 2$.

5. Subsequent immersions in NH_4Cl, NH_4OH and (anaerobic) KCN lead to the conclusion that the presence of Cu_nS_m, $1 \leq n/m \leq 2$, on the surface is necessary for the device to operate as a solar cell.

THEORETICAL STUDY OF THE PHOTOVOLTAIC CELL

Theory of the Surface Barrier Photovoltaic Effect

In this section we propose a model for the mode of operation of a surface barrier photovoltaic cell, and outline the methods used for the theoretical estimation of its output. Specifically we postulate the following sequence. Consider a surface on which a density of surface traps, N_t, is located at an energy E_t. These traps are considered to be in communication with the valence and conduction bands; their behavior is characterized by two capture cross sections, C_p for holes and C_n for electrons. Given this situation, we consider the following sequence:

1. In the dark, in equilibrium, the traps N_t will be fractionally populated by a density of electrons determined by the Fermi function, irrespective of the values C_p and C_n.

2. The states, or traps, N_t will have a net charge in this situation. Specifically this net charge we take to be $(-qfN_t)$, where $-q$ is the electronic charge, and f the value of the Fermi function.

3. This net charge gives rise to a surface barrier extending into the bulk for a distance determined by the Debye length.

4. Upon illumination of the cell, excess carriers are created. A recombination process occurs, in part via the surface traps. In the steady state condition, neither the carrier concentration nor the charge in surface traps are equal to those in equilibrium. Particularly, the charge in the surface states changes, and also tha barrier height and its nature change.

5. The change in barrier height is taken to be the voltage output of the cell.

We are able to estimate the voltage output for open circuit conditions by the analysis in Figure 21.

In thermal equilibrium the concentrations of electrons and holes are

$$n_0 = n_i \exp -q(\phi - \psi)/kT$$

$$p_0 = n_i \exp -q(\psi - \phi)/kT$$

where $\psi = \psi(x)$ in general.

In the steady state, upon illumination, the actual concentrations are given by

$$n = n_i \exp -q(\phi_n - \psi)/kT$$

$$p = n_i \exp -q(\psi - \phi_p)/kT$$

where ϕ_n and ϕ_p are the electron and hole quasi-fermi levels, related to the original fermi level by

$$\phi_n = (\phi - \Delta\phi_n)$$

$$\phi_p = (\phi - \Delta\phi_p)$$

In Figure 21 electron energy is plotted upwards, and therefore potential is plotted downwards. $\Delta\phi_n$ and $\Delta\phi_p$ are positive in the directions indicated by the arrows denoting them in Figure 21.

It follows that

$$n = n_0 \exp \Delta\phi_n \, q/kT$$

$$p = p_0 \exp \Delta\phi_p \, q/kT.$$

For convenience, define:

$$u = q(\psi - \phi)/kT,$$

$$\Delta u_n = \Delta\phi_n \, q/kT,$$

$$\Delta u_p = \Delta\phi_p \, q/kT,$$

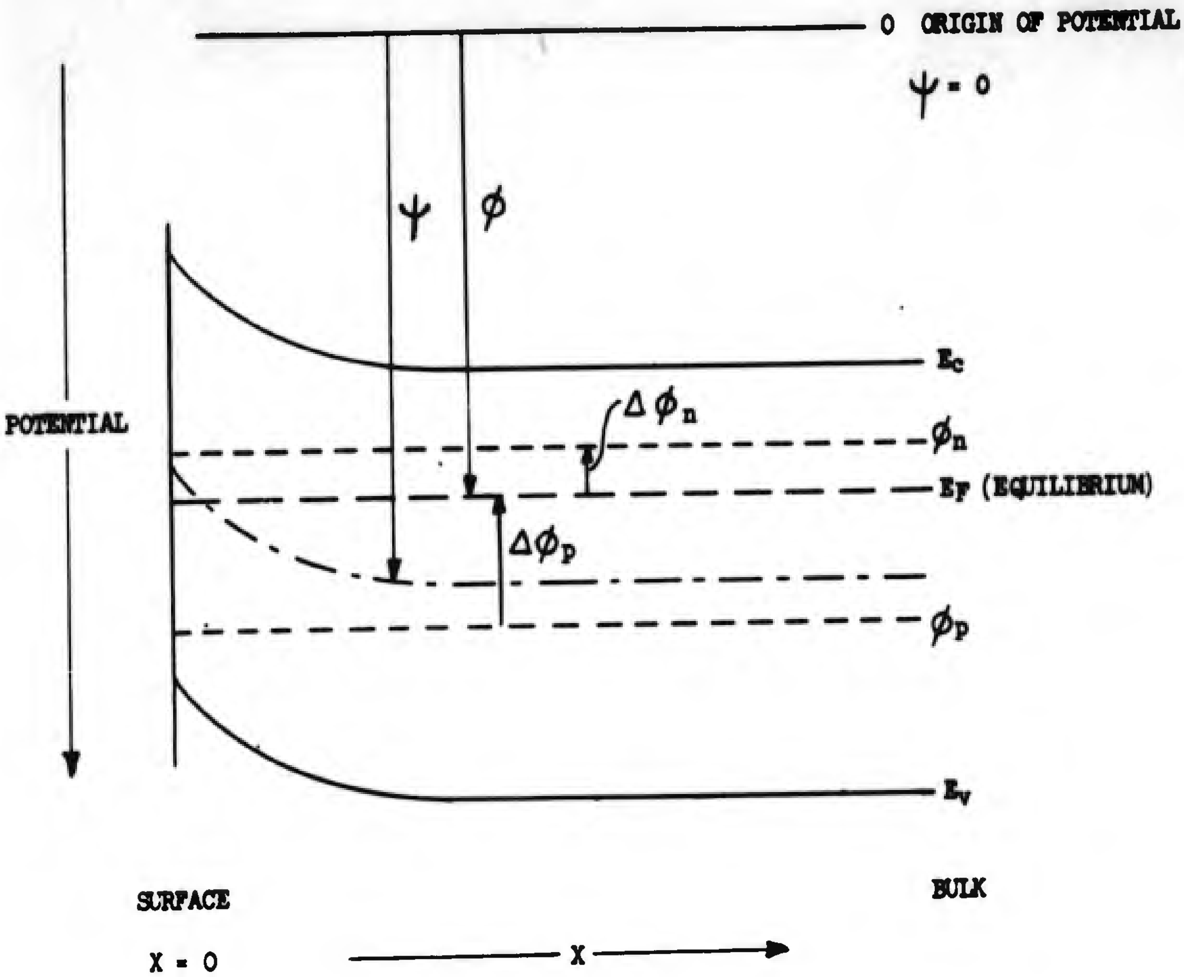

FIGURE 21

Energy Level Diagram-Surface Barrier Photovoltaic Cell
(Energy Bands Near The Surface Of A Semi-conductor Under Illumination)

$$L_D^{\,2} = K\epsilon_0\, kT/2q^2 ni,$$

where $K\epsilon_0$ is the permittivity of the material. We may now write Poisson's equation in terms of a charge density

$$\nabla^2\psi = -\rho/K\epsilon_0$$

where

$$\rho = q(N_D - N_A + p - n),$$

in which N_D, N_A are the densities of donors and acceptors.

Poisson's equation reduces to

$$\frac{\partial^2\psi}{\partial x^2} = -\Big[\exp(-u + \Delta u_p) - \exp(u + \Delta u_n) - \exp(-u_B) + \\ + \exp u_B\Big]/2L_D^{\,2},$$

where u_B is the constant value of u deep in the bulk.

A first integration gives

$$L_D \frac{\partial u}{\partial x} = F = \Big[\exp\Delta u_p\ (\exp(u_s - 2u_B) - 2\exp u_B + \\ + \exp\ -u_s) + \exp u_s\,(1 - \exp -2u_B) - \\ - (\exp u_B - \exp - u_B\,(1 + u_s - u_B)\ )\Big]^{\frac{1}{2}}$$

where u_s is the value of u at $x = 0$, and in which we have eliminated Δu_n by the consideration that

$$n = n_0 + \delta n$$

$$p = p_0 + \delta p$$

and if $\delta n = \delta p$, it can be shown that

$$\exp\Delta u_n = \exp - 2u_B\,(\exp 2u_B - 1 + \exp\Delta u_p)$$

The electric field at the surface is

$$E_s = -\left(\frac{\partial \psi}{\partial x}\right)_{x=0} = (kT/qL_D)\ F.$$

This electric field corresponds to a net charge in the material of Q where

$$Q = K\epsilon_0\ (kT/qL_D)\ \ F,$$

or to a charge in surface states of -Q.

Let us now pay attention to the charge in surface states. Following Shockley and Read, we write the charge in curface states of density N_t as

$$-Q = qN_t f_t$$

$$= -qN_t\ (C_n n_s + C_p p_i \ / \ C_p(p_i + p_s) + C_n(n_s + N_i)$$

where n_s, p_s are the carrier concentrations at the surface, and the other symbols have their usual meaning.

In our notation this reduces to

$$-Q = N_t q f_t$$

$$= -N_t\ q\left[1 + \frac{Re^{u_t} + e^{(-u_s - \Delta u_B)}}{Re^{u_s}\ (1-e^{-2u_B} + e^{-2u_B + \Delta u_p}) + e^{-u_t}}\right]^{-1}$$

where R is the ratio C_n/C_p and u_t is the trap potential, measured in units of (kT/q).

Equating the moduli of these two values for Q, we have

$$N_t q\left[1 + \frac{Re^{u_t} + e^{(-u_s - \Delta u_B)}}{R \exp u_s\ (1- \exp - 2u_B + \exp\ (-2u_B + \Delta u_p) + \exp -u_t}\right]^{-1}$$

$$= K\epsilon_o (kT/qL_o)\Big[\exp\Delta u_p (\exp u_s - 2u_B - 2\exp - u_B + \exp -u_s) + + \exp u_s (1 - \exp - 2u_B) - (\exp + u_B - \exp u_B)(1 + u_s - u_B)\Big]^{\frac{1}{2}},$$

which we may write

$$N_t qH = K\epsilon_o \frac{(kT)}{(qL_D)} F.$$

This equation may be solved for u_s for any given value of $\Delta\phi p$ (i.e. light intensity). The barrier height equals $(u_B - u_s)$ and the change in barrier height then is clearly equal to the change in u_s as $\Delta\phi$ p, or the light intensity, is changed. The expressions involved are quite complicated, so a graphical method of solution must be employed..

The theory presented so far refers specifically to the open circuit voltage of the cell. Of equal importance is the estimation of the short circuit current. At present no known method for this computation is available; in the absence of a conventional approach, an attempt was made to estimate the short circuit current on the basis of a hypothesis regarding the nature of the current flow into a barrier region from a surface layer. As will be seen in the following section, this hypothesis intimately limits the short circuit current, the ohmicity of the contact (from the point of view of carrier concentration disturbance) and the surface recombination velocity.

A Hypothesis on Injecting Contacts

It is well known that any given metal semiconductor contact may be ohmic or non-ohmic, and may change the local carrier concentration in four ways(19) characterized by the contact being:

1. Injecting,
2. Excluding,
3. Exhausting,
4. Accumulating.

There is no coherent model available to account for these phenomena, which may occur, apparently haphazardly, at a contact that is nominally believed to be otherwise uniquely defined. In order to construct a model, the following hypothesis has been made.

Given a surface, consider that a density N_t of surface traps occur at energy E_t, and are characterized by cross sections C_p and C_n, for electrons and holes, respectively. A fraction f, of the N_t traps will be filled, and so a charge $(-qfN_t)$ is assigned to them. This charge, in equilibrium, gives rise to a barrier(20,21) at the surface of the semiconductor. Now hypothesize that the metal to semiconductor contact is made <u>via</u> the surface states N_t, either directly or indirectly if a second barrier is considered. In the steady state, a current I is assumed to flow into the surface states, and their occupancy is changed from f to $(f + \delta f)$. Under these conditions, the charge in the surface states is $-q(f + \delta f)N_t$; a new barrier height results.

Following Shockley and Read$^{(22)}$, the rate of capture of electrons and holes by the surface states is

$$U_{cn} = C_n(1-f)n_s - C_n f\, n_1$$

$$U_{cp} = C_p f\, p_s - C_p(1-f)\, p_1.$$

Here n_s, p_s, are the surface concentration of electrons and holes, and n_1, p_1, are two constants which depend on the band gap and on the position of the Fermi level. In the steady state these equations become

$$U'_{cn} = Cn(1-f-\delta f)(n_s+\delta n_s) - Cn(f+\delta f)n_1$$

$$U'_{cp} = Cp(f+\delta f)(p_s+\delta p_s) - Cn(1-f-\delta f)p_1$$

where $(n_s + \delta n_s)$ and $(p_s + \delta p_s)$ are the new surface concentrations of electrons and holes.

The electron current into the traps is $U'_{cp} - U'_{cn}$,(if this quantity is negative it indicates a flow out of the traps). The quantity becomes, after setting $U_{cp} = U_{cn}$ (the thermal equilibrium case),

$$(U'_{cp} - U'_{cn}) = C_p(\delta f\, (p_s + \delta p_s) + \delta p_s f + \delta f_{p_1}) +$$

$$+ C_n\, (\delta f\, (n_s + \delta n_s) - (1-f)\, \delta n_s + \delta f_{n_1}).$$

As an illustration of the application of this result, two particular cases will be briefly discussed, pertaining to "n" type material.

I. Weak "n" barrier, i.e., in which the surface is slightly weaker than the bulk. This means that only a small charge exists on the surface, which in turn suggests that $E_t \rightarrow E_c$, the energy of the conduction band.

The ratio

$$\frac{\text{Minority current from traps}}{\text{Majority current from traps}}$$

will be formed. It is:

$$R = \frac{Ucp - U'cp}{Ucn - U'cn}$$

$$= \frac{-C_p\,(\delta f\,(p_s + \delta p_s) + \delta p_s f + \delta f_{p_1})}{C_n\,(\delta f\,(n_s + \delta n_s) - (1-f)\delta n_s + f_{n_1})},$$

generally.

In this case,

$$R = \frac{-C_p}{C_n}\;\frac{\delta f\,(p_s + \delta p_s) + \delta p_s f}{\delta f\,(n_s - \delta n_s) + (1-f)\delta n_s + \delta f_{n_1}} =$$

$$= \frac{C_p}{C_n}\;\frac{(p_s + \delta p_s)}{n_1} \rightarrow 0.$$

In other words, in the case of a weak "n" barrier on an "n" type material, we expect that negligible minority carrier current flows into the material; it is therefore non-injecting.

II. Strong "p" barrier on "n" type material. This means that the surface charge is strongly negative, and f ⟶ 1, and $E_t \longrightarrow E_v$. Therefore,

$$R \doteq \frac{C_p}{C_n}\;\frac{\delta f p_s + \delta f_{p_1}}{(f + \delta f - 1)\,\delta n_s},$$

which is large in this case, and can be positive or negative. It is therefore to be expected that in this case there is strong injection (or exclusion). It must be further remarked that the two cases (I) and (II) can, from the work of Stevenson and Keyes(23), be correlated with various values of surface recombination velocity. Case (I) is assigned by those authors to be that for strong surface recombination, and case (II) is that for weak surface recombination.

In all the examples considered, it has been found that the hypothesis presented here suggests that carrier concentrations are disturbed least when it would be expected that the surface conditions were those suitable for maximum surface recombination velocity, and *vice versa*. This association is known to exist experimentally. It can be said, therefore, that the results of the hypothesis are in qualitative agreement with the facts.

Applications to the CdS Photovoltaic Cell

In retrospect, the theory applicable to the open circuit voltage has been formulated. The mode of operation was postulated to be as follows:

(I) A set of recombination centers was assumed to exist on the surface of the material, being fractionally populated to an extent f.

(II) The charge in the centers (or traps) gave rise to a barrier.

(III) Upon illumination of the bulk material, excess concentrations arose in the bulk, and recombination occurred via the surface states.

(IV) In the recombination process, the charge in the surface states altered, altering in turn the barrier height.

(V) The change in barrier height, upon illumination, was equal to the open circuit voltage of the cell.

Now consider the case of the short circuit current. Assume that an excess carrier concentration is built up, upon illumination, by about 10^{10} carriers/cm^3. Further, assume that the base material of a photovoltaic cell is of such low resistivity that any resistance there may be neglected, i.e. the slope of quasi Fermi levels may be neglected.

For CdS of low resistivity, the Fermi level may be assumed to be 45 units of kT/q above the mid-gap position, and using the model assumed in reference (22), the Fermi level may be taken as being, in complete darkness, at nearly the intrinsic position. These figures correspond to 10^{18} electrons/cm^3 in the bulk, and negligible concentration at the surface. In both cases the holes are of negligible importance. Now let the barrier be illuminated so as to increase the local concentrations there by 10^{10} (this assumes an incident flux of 10^{16} photons/sec on the barrier, and a lifetime of 10^{-6} seconds is effective). Therefore,

$$\delta p_s = 10^{10}$$

at the surface.

The total flow into the surface states may now be computed; it is assumed that short circuit conditions prevail, so there is no change in barrier height (therefore $\delta f = 0$), and the traps are approximately at mid gap energies, so that $f \sim \frac{1}{2}$, and n_1 and p_1 are both negligible.

Therefore, $U'_{cp} - U'_{cn}$ is of the order of $C_p/2 \cdot \delta p_s$, and is of course, the total current flowing out of the cell. C_p is defined as being negative and is given approximately by the relation: $C_p = N_t A v$, where A is the capture cross section of an individual trap and v is the thermal velocity of the carriers. Reasonably, A may be equated to the cross section area of an atom (10^{-15} cm^2) and v is approximately 10^7 cm/sec. N_t is taken as 10^{14}/cm^2. The electron flow is of the order

$$C_p \delta p_s = 10^{14} \times 10^{-15} \times 10^7 \times 10^{10} \text{ electron/sec}$$

$= 10^{16}$ electrons/sec

$= 10^{-3}$ coulombs/sec, referred to 1 cm^2.

While it is realized that many coarse assumptions have been made in this analysis, it is encouraging that the theoretical figure agrees moderately well with the actual output of a CdS photovoltaic cell. It is felt that there are therefore sufficient grounds for pursuing this model further, and making whatever refinements are necessary.

The Barrier Capacity

The model presented differs in no serious way from a p-n junction insofar as the capacity of the device is concerned. In both cases, the p-n junction and the surface barrier, there is effectively a double layer of charge separated by a thickness of the order of a barrier depth. This depth is in turn of the order of the effective Debye Length, which is defined as

$$L_D{}^2 = \frac{K \epsilon_0 kT}{2q^2 n}$$

where n is the actual concentration of carriers. We take the figure for L_D to be of the order of 10^{-5}cm, and get therefore a device capacitance in the range 10^{-8} to 10^{-7} farads (per cm^2). As has been stated, this figure is governed largely by the material, and not by the particular mechanism of double layer formation, i.e. it does not distinguish between a p-n junction and a surface barrier. It is not surprising, therefore, that the measured capacity is of this order (ref. 16, Pg. 50-57).

The surface barrier model, however, does give an additional figure which may help in associating that particular model with the actual physical configuration. Consider the following argument. The measured and the predicted short circuit current is about 10^{-3} amps/cm^2. It has been assumed that the traps responsible for the cell action are in roughly the mid gap position, i.e. of the order of one volt from the band edge.

It is possible, therefore, to assign a "pumping resistance" to the cell; namely, the band-to-trap energy divided by the short circuit current. This resistance is of the order of 10^3 ohms.

Summary of Cell Operation

The self consistencies of the surface barrier model make it an extremely attractive assumption. It is readily argued that front-wall and back-wall modes of operation are possible, and may have different characteristics. The main features of operation may be summarized.

Back Wall Operation

V_{oc}:

a. Carrier excitation in the bulk
b. Recombination at the surface
c. Change in surface state occupancy
d. Change in barrier height

I_{sc}:

a. Carrier excitation in the bulk
b. Contact to barrier maintains constant occupancy of surface states
c. Steady state recombination processes lead to excess electron capture, and hence to a current output

Front Wall Operation

V_{oc}:

a. Carrier excitation from surface states
b. Surface state occupancy unchanged
c. Recombination processes lead to excess electron capture

It is to be noted that the front wall operation is extremely similar to the model proposed by Bube and Williams.(24)

PART III - RECOMENDATIONS

Separate recommendations have been made in a proposal for continuation of the development and research phases of semiconducting CdS for large area light weight photovoltaic devices.

The purity of starting materials for either single crystal of film growth remains an unknown factor in the measurement and control of electrical characteristics. This arises at this time because of the discovery of small amounts of Na and other alkali and alkali earth metals by mass spectrometry, and of oxygen in a variety of raw materials and under a variety of conditions in cell preparation. To determine quantitatively the effect of these impurities on the electrical and optical properties of CdS crystals and cells, a thorough program of purification and analysis is strongly suggested.

Once a really ultrahigh purity CdS material is obtained, a second large area of research problems could be investigated with more assurance of fruitful results. Thus, the influence of dislocations and crystal or crystallite orientation could be directly ascertained without the complications of extraneous electrically active impurities. The isolation and study of certain types of dislocations would be placed on a firm experimental basis. Also, efforts could then be made to optimize doping to obtain selected trapping levels in the forbidden gap, thus tailoring the spectral response of cells to the solar spectrum to reach higher levels of conversion efficiency.

Cell developmental efforts should include a major effort to improve the structure and physical perfection of evaporated films so that very thin films could be used to obtain truly light weight flexible cells of high efficiency. Also, improved methods of treating films by annealing in various atmospheres and in the presence of certain impurities may lead to the attainment of larger crystallites and more perfect structure, and variations in the methods of "disturbing" film surfaces may lead to increased density of activation centers.

Increased attention to the conditions of substrate preparation, film evaporation and barrier formation is needed to improve the reproducibility of film cell fabrication leading to the economical manufacture of large area efficient photovoltaic cells possessing high ratios of power per unit of weight.

Since little is known about the barrier in CdS cells, other than its probable composition, it is recommended that more detailed study of the barrier be made; including its attachment to the CdS surface, optimum methods of formation, and the effects of heat, water vapor and oxygen.

Two major approaches to understanding and improving the CdS barrier from the physics point of view are believed worthwhile at this time. The first is the experimental verification of the theory associating open circuit voltage with the change in contact potential. A direct experimental study of the change in contact potential with light on CdS surfaces should be made as a function of surface treatment and ambient. The second is the assignment of a mechanism to the barrier contact explaining the short circuit current and relating the surface recombination velocity to the ohmicity of the contact.

Factors influencing the stability of barriers on CdS crystals should be studied in detail including the effects of radiation as well as atmospheric effects. Methods of protecting the cells from degradation should be developed and extended life tests run. Techniques must be developed further for mounting CdS film cells in light weight arrays suitable for packaging for launching in satellite vehicles and unfurling in space.

REFERENCE LIST

1. Shirland, F.A.: "Photovoltaic Cadmium Sulfide," ARL Technical Report 60-293, pg. 4 (Aug., 1960).

2. Ibid, Pgs. 25-35.

3. Devlin, S.S.; Jost, J.M.; and Shiozawa, L.R.: "Research on New High Temperature Semiconducting Materials," WADD Technical Report 60-11, Pgs. 99-103 (April, 1960).

4. Carlson, A.: "Research on Semiconductor Films," WADC Technical Report 56-52, (Jan., 1956).

5. Shirland, F.A. and Gorski, D.A.: "Research on a Composite Energy Gap Photovoltaic Cell," Third Quarterly Progress Report, Contract Nr. AF33(616)-6548, (March, 1960).

6. Jaffe, M.S.: "Indium Basic Trifluoracetate and Method of Coating Bodies Therewith," U.S. Patent No. 2,849,339 (1958).

7. Ennos, A.E.: "Highly-Conducting Gold Films Prepared by Vacuum Evaporation," BRIT. J. APPL. PHYS., 8, pgs. 113-117 (1957).

8. Rindner, W., and Lavine, J.M.: "Scribe-Plating and Etching," J. ELECTROCHEMICAL SOC., 108, pgs. 869-873 (1961).

9. Kroger, F.A.; Vink, H.J. and van den Boomgaard, J.: "Controlled Conductivity in CdS Single Crystals," Z. PHYSIK. CHEM., 203, 1-72 (1954).

10. Czyzak, S.J.; Craig, D.J.; McCain, C.E. and Reynolds, D.C.: "Single Synthetic CdS Crystals," J. APPL. PHYS., 23, pgs. 932-933 (1952).

11. Gordon, A.R.: private communication quoted in H. Zeise: "Spectrophysics and Thermodynamics," Z. ELEKTROCHEM., 40, pgs. 885-890 (1934).

12. Wolff, G.A.; Wilbur, J.M. Jr.; Clark, J.C.: "Etching and Orientation Measurements of Diamond Type Crystals by Means of Light Figures," ZEIT. FUR ELEKTROCHEMIE - Berichte der Bunsengesellschaft fur Physikalische Chemie; Band 61, Heft 1, pgs. 101-106 (1957).

13. Gilles, J.H. and Van Cakenberghe, J.: "Photoconductivity and Crystal Size in Evaporated Layers of CdS," NATURE, 182, pgs. 862-863 (1958).

14. Reynolds, D.C. and Greene, L.C.: "Crystal Growth Mechanism in CdS Crystals," J. APPL. PHYS., 29, pgs. 559-562 (1958).

REFERENCE LIST (Continued).

15. Woods, J.: "Etch Pits and Dislocations in Cadmium Sulfide Crystals," BRIT. J. APPL. PHYS., 11, pgs. 296-302, (1960).

16. Shirland, F.A.: "Photovoltaic Cadmium Sulfide," ARL Technical Report 60-293, pgs. 42, (Aug., 1960).

17. Saubestre, E.B.: "Electroless Copper Plating," Proc. Amer. Electroplaters Soc., pgs. 264-276 (1959).

18. Shirland, F.A.; Wolff, G.A.; Nixon, J.D.: "Fourth Quarterly Progress Report," This Contract, pgs. 46-49 (July 20, 1961).

19. Low, G.G.E.: "Carrier-Concentration Disturbances in Semiconductors," PROC. PHYS. SOC., (London) B.68, pgs. 310-314 (1955).

20. Kingston, R.H.: "Review of Germanium Surface Phenomena," J. APPL. PHYS., 27, pgs. 101-114 (1956).

21. Shirland, F.A.; Wolff, G.A.; Nixon, J.D.: "Third Quarterly Progress Report," Contract AF33(616)-7528 (April 28, 1961).

22. Shockley, W. and Read, W.T.: "Statistics of the Recombinations of Holes and Electrons," PHYS. REV., 87, pgs. 835-842 (1952).

23. Stevenson, D.T. and Keyes, R.J.: "Measurements of the Recombination Velocity at Germanium Surfaces," PHYSICA, 20, pg. 1041 (1954). Many, A.; Harnik, E. and Margoninski, Y.: "Surface Recombination Processes in Germanium and Their Investigation by Means of Transverse Electric Fields," SEMICONDUCTOR SURFACE PHYSICS, University of Pennsylvania Press, Philadelphia; pgs. 85-107 (1956).

24. Williams, R. and Bube, R.H.: "Photoemission in the Photovoltaic Effect in Cadmium Sulfide Crystals," J. APPL. PHYS., 31, pgs. 968-978 (1960).

25. Gualtieri, J.G.; Katz, M.J. and Wolff, G.A.: "Gas Etching and Its Effect on Semiconductor Surfaces," Z. KRIST, 114, pgs. 9-22 (1960).

Aeronautical Systems Division, Dir/Aeromechanics, Flight Accessories Lab, Wright-Patterson AFB, Ohio. Rpt Nr ASD-TDR-62-69. RESEARCH ON SOLAR-ENERGY CONVERSION EMPLOYING CADMIUM SULFIDE. Summary report, June 62, 73p. incl illus., tables, 25 refs.

Unclassified Report

Application of CdS to photovoltaic conversion has been continued with primary emphasis on cells fabricated from vacuum evaporated CdS films. Back wall CdS film cells on conducting glass substrates have given efficiencies up to 5% on small areas. Front wall CdS film cells on molybdenum foil substrates have given efficiencies up to 2.5% on small areas and up to 1.0% on larger areas of 9 in^2. Thin lightweight arrays have been constructed from the latter cells having power to

(over)

1. Solar cells
2. Photovoltaic materials
3. Solar energy conversion
4. Semiconductors

I. AFSC Project 3145, Task 314508
II. Contract AF33(616)-7528
III. Harshaw Chem. Co., 2240 Prospect Ave., Cleveland 15, Ohio
IV. F.A. Shirland, G.A. Wolff and J.D. Nixon
V. Aval fr OTS
VI. In ASTIA collection

weight ratios up to 10 watts per pound. Improvements promising increases up to 30 to 40 watts per pound are discussed. Arrays of CdS film cells of 1 square foot area have been constructed. Fundamental investigations were initiated on the growth, annealing, etching, and orientation of CdS single crystals and films. The results were correlated with the type of crystal imperfection and its probable influences on electrical properties. The photovoltaic barrier was studied experimentally to identify the essential constituents and to improve the expected efficiency of energy conversion. Theoretical models were postulated for the mechanisms occurring in the CdS photovoltaic cell.

Aeronautical Systems Division, Dir/Aeromechanics, Flight Accessories Lab, Wright-Patterson AFB, Ohio. Rpt Nr ASD-TDR-62-69. RESEARCH ON SOLAR-ENERGY CONVERSION EMPLOYING CADMIUM SULFIDE. Summary report, June 62, 73p. incl illus., tables, 25 refs.

Unclassified Report

Application of CdS to photovoltaic conversion has been continued with primary emphasis on cells fabricated from vacuum evaporated CdS films. Back wall CdS film cells on conducting glass substrates have given efficiencies up to 5% on small areas. Front wall CdS film cells on molybdenum foil substrates have given efficiencies up to 2.5% on small areas and up to 1.0% on larger areas of 9 in^2. Thin lightweight arrays have been constructed from the latter cells having power to

(over)

1. Solar cells
2. Photovoltaic materials
3. Solar energy conversion
4. Semiconductors

I. AFSC Project 3145, Task 314508
II. Contract AF33(616)-7528
III. Harshaw Chem. Co., 2240 Prospect Ave., Cleveland 15, Ohio
IV. F.A. Shirland, G.A. Wolff and J.D. Nixon
V. Aval fr OTS
VI. In ASTIA collection

weight ratios up to 10 watts per pound. Improvements promising increases up to 30 to 40 watts per pound are discussed. Arrays of CdS film cells of 1 square foot area have been constructed. Fundamental investigations were initiated on the growth, annealing, etching, and orientation of CdS single crystals and films. The results were correlated with the type of crystal imperfection and its probable influences on electrical properties. The photovoltaic barrier was studied experimentally to identify the essential constituents and to improve the expected efficiency of energy conversion. Theoretical models were postulated for the mechanisms occurring in the CdS photovoltaic cell.

Aeronautical Systems Division, Dir/Aeromechanics, Flight Accessories Lab, Wright-Patterson AFB, Ohio. Rpt Nr ASD-TDR-62-69. RESEARCH ON SOLAR-ENERGY CONVERSION EMPLOYING CADMIUM SULFIDE. Summary report, June 62, 73p. incl illus., tables, 25 refs.

Unclassified Report

Application of CdS to photovoltaic conversion has been continued with primary emphasis on cells fabricated from vacuum evaporated CdS films. Back wall CdS film cells on conducting glass substrates have given efficiencies up to 5% on small areas. Front wall CdS film cells on molybdenum foil substrates have given efficiencies up to 2.5% on small areas and up to 1.0% on larger areas of 9 in^2. Thin lightweight arrays have been constructed from the latter cells having power to

(over)

1. Solar cells
2. Photovoltaic materials
3. Solar energy conversion
4. Semiconductors

I. AFSC Project 3145, Task 314508
II. Contract AF33(616)-7528
III. Harshaw Chem. Co., 2240 Prospect Ave., Cleveland 15, Ohio
IV. F.A. Shirland, G.A. Wolff and J.D. Nixon
V. Aval fr OTS
VI. In ASTIA collection

weight ratios up to 10 watts per pound. Improvements promising increases up to 30 to 40 watts per pound are discussed. Arrays of CdS film cells of 1 square foot area have been constructed. Fundamental investigations were initiated on the growth, annealing, etching, and orientation of CdS single crystals and films. The results were correlated with the type of crystal imperfection and its probable influences on electrical properties. The photovoltaic barrier was studied experimentally to identify the essential constituents and to improve the expected efficiency of energy conversion. Theoretical models were postulated for the mechanisms occurring in the CdS photovoltaic cell.

Aeronautical Systems Division, Dir/Aeromechanics, Flight Accessories Lab, Wright-Patterson AFB, Ohio. Rpt Nr ASD-TDR-62-69. RESEARCH ON SOLAR-ENERGY CONVERSION EMPLOYING CADMIUM SULFIDE. Summary report, June 62, 73p. incl illus., tables, 25 refs.

Unclassified Report

Application of CdS to photovoltaic conversion has been continued with primary emphasis on cells fabricated from vacuum evaporated CdS films. Back wall CdS film cells on conducting glass substrates have given efficiencies up to 5% on small areas. Front wall CdS film cells on molybdenum foil substrates have given efficiencies up to 2.5% on small areas and up to 1.0% on larger areas of 9 in^2. Thin lightweight arrays have been constructed from the latter cells having power to

(over)

1. Solar cells
2. Photovoltaic materials
3. Solar energy conversion
4. Semiconductors

I. AFSC Project 3145, Task 314508
II. Contract AF33(616)-7528
III. Harshaw Chem. Co., 2240 Prospect Ave., Cleveland 15, Ohio
IV. F.A. Shirland, G.A. Wolff and J.D. Nixon
V. Aval fr OTS
VI. In ASTIA collection

weight ratios up to 10 watts per pound. Improvements promising increases up to 30 to 40 watts per pound are discussed. Arrays of CdS film cells of 1 square foot area have been constructed. Fundamental investigations were initiated on the growth, annealing, etching, and orientation of CdS single crystals and films. The results were correlated with the type of crystal imperfection and its probable influences on electrical properties. The photovoltaic barrier was studied experimentally to identify the essential constituents and to improve the expected efficiency of energy conversion. Theoretical models were postulated for the mechanisms occurring in the CdS photovoltaic cell.